

620921335  
TK  
1541  
1344  
2010

# **FAULT RIDE THROUGH CAPABILITY OF DOUBLE FED INDUCTION GENERATOR FOR WIND ENERGY SYSTEM**

By

Hussien Berisso, BEng

Ryerson University, 2007

A Master's Project Report

presented to Ryerson University

in partial fulfillment of the

requirements for the degree of

Master of Engineering in the program of

Electrical and Computer Engineering

Toronto, Ontario, Canada 2010

© Hussien Berisso 2010

I hereby declare that I am the sole author of this report.

I authorize Ryerson University to lend this report to other institutions or individuals for the purpose of scholarly research.

Signature

I further authorize Ryerson University to reproduce this report by photocopying or by other means, in total or in part, at the request of other institutions or individuals for the purpose of scholarly research.

Signature



## ABSTRACT

Until recently it has been accepted that induction generator based wind turbines are disconnected from the power system in the event of a network disturbance. However, the increasing trend of connecting high penetrations of wind farms to transmission networks has resulted in the transmission system operators revising their grid codes for the connection of large MW capacity wind farms. The new grid codes require wind turbines to remain connected for a specified voltage disturbance on the network. Most of the wind generation plant being developed will use either fixed speed induction generator (FSIG) or doubly fed induction generator (DFIG) based wind turbines. The basics of using a doubly-fed induction generator (DFIG) to convert the mechanical energy of the wind into useful electrical power that can be used to supply electricity to any grid are presented. The ability of doubly fed induction generator based wind turbines to remain connected through power system disturbances is discussed. A crowbar protection system to provide a power system fault ride-through capability for doubly fed induction generator based wind turbines is also described. The dynamic behaviour of DFIG wind turbines normal operation and during grid faults are simulated and assessed to verify the recommended method using a Matlab/Simulink developed model.

## **ACKNOWLEDGEMENTS**

I wish to express my deep gratitude to my academic supervisor, Professor Bin Wu for his support and guidance and the knowledge he shared during my graduate studies at Ryerson University and Wroclaw University of Technology in Poland.

I would like to also thank the faculty and staff of Wroclaw University of Technology, department of electrical power engineering, for their continuous guidance during my one year study in Poland.

And last but not least I would like to give my deepest thanks to my siblings, whose presence, constant support and understanding made this work possible.

# TABLE OF CONTENTS

CHAPTER 1 INTRODUCTION.....	1
1.1 Background.....	1
1.2 Wind Energy Conversion Systems.....	3
1.3 Low Voltage Ride through (LVRT).....	7
1.4 Motivation.....	11
1.5 Report Outline.....	13
CHAPTER 2 MODEL AND OPERATING PRINCIPLE OF DFIG.....	13
2.1 Modeling of DFIG.....	16
2.2 Rotor Side Converter.....	20
2.3 Grid Side Converter.....	23
2.4 DFIG Normal Operation Analysis.....	24
2.5 Summary.....	28
CHAPTER 3 FAULT ANALYSIS OF DFIG.....	29
3.1 DFIG During Fault.....	30
3.2 Three Phases Shorted to Ground Fault.....	31
3.3 Two Phases shorted Fault.....	33
3.3 Summary.....	35
CHAPTER 4 FAULT DETECTION AND PROTECTION.....	36
4.2 Introduction .....	36
4.2 Fault Detection Methods.....	37
4.3 Protection using Active Crowbar.....	38
4.4 Summary.....	47
CHAPTER 5 CONCLUSIONS.....	48
5.1 Conclusion.....	49
5.2 Major Contributions.....	50

REFERENCES.....	51
APPENDIX .....	54

## LIST OF FIGURES

Figure 1-1 Worldwide wind energy capacity prediction, 2008.....	2
Figure 1-2 Power coefficient, $C_p$ , as a function of the tip speed ratio, $\lambda$ .....	5
Figure 1-3 The turbine power, the tip speed ratio $\lambda$ and the $C_p$ .....	6
Figure 1-4 Low ride- through voltage charactersics.....	9
Figure 2-1 General operating model of DFIG with converters .....	15
Figure 2-2 Power flow diagram of DFIG.....	15
Figure 2-3 Equivalent circuit of Doubly Fed Induction Generator.....	18
Figure 2-4 The rotor speed and active power control diagram.....	21
Figure 2-5 Doubly fed induction generator with converters connected to a Grid.....	22
Figure 2-6 Reactive power and voltage control diagram.....	23
Figure 2-7 DFIG normal operation.....	26
Figure 3-1 DFIG Characteristics during a 3 phase fault.....	32
Figure 3-2 DFIG Characteristics during a 2- phase fault.....	34
Figure 4-1 Diode bridge crowbar.....	39
Figure 4-2 DFIG structure with active crowbar.....	40
Figure 4-3 Control block of DFIG with a crowbar.....	41

Figure 4-4 DFIG during fault without crowbar.....	43
Figure 4-5 Stator and rotor current and electromagnetic torque during fault without crowbar.....	44
Figure 4-6 Stator and rotor current and electromagnetic torque during fault with crowbar.....	45
Figure 4-7 Stator and rotor voltage and DC-link voltage during fault with the crowbar.....	45



# CHAPTER 1

## INTRODUCTION

### 1.1 Background

Energy from the sun, in the form of wind, plant matter, and heat and light, is renewable. Renewable energy offers a clean, cost effective alternative to fossil fuels and nuclear power. Producing power from these renewable sources can be far less environmentally damaging than conventional energy sources. Wind energy, more than any other renewable energy technology, is a proven, non-polluting renewable resource that is beginning, and will continue, to play an important role in meeting the rising energy demands.

People have harnessed the wind throughout history to convert wind energy into useable energy. Less than 100 years ago, millions of small windmills provided an important source of power for rural homes. These machines powered water pumps and converted wind into electricity. Beginning in the 1930s, rural electrification programs began to extend the electrical grid into the countryside, replacing wind energy with electricity generated from fossil fuels and large hydroelectric projects. The once abundant wind machines that were a common feature of the rural landscape have largely disappeared from sight [3].

Today, however, new wind machines are beginning to appear on the landscape, as windy rural areas tap a unique opportunity to benefit from wind power. Modern wind turbine technology now makes it possible to generate cost-effective, clean, renewable electricity on a scale ranging from a single wind turbine for an individual landowner up to large, utility-scale wind farms. Declining costs and improving technology are quickly making electricity generated from wind energy competitive with all types of non-renewable fuels, like new coal-fired generation. The price of wind generated electricity has decreased ten times since the early 1980s, to the point that the American Wind Energy Association estimates that within three to four decades, wind power could realistically supply ten to twenty percent of developed countries need.[1,4]

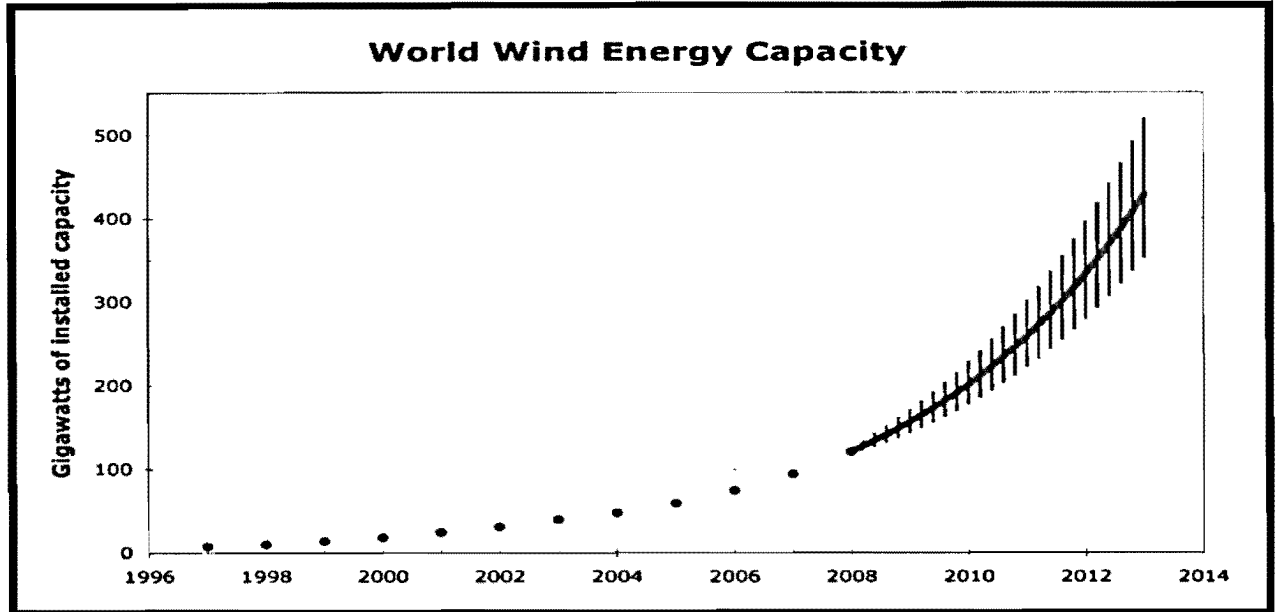


**Fig. 1-1 Worldwide wind energy capacity prediction, 2008 [3].**

Since wind speed is not constant, a wind farm's annual energy production is never as much as the sum of the generator nameplate ratings multiplied by the total hours in a year. The ratio of actual productivity in a year to this theoretical maximum is called the capacity factor. Typical capacity factors are 20–40%, with values at the upper end of the range in particularly favourable sites. For example, a 1 MW turbine with a capacity factor of 35% will not produce 8,760 MW·h in a year ( $1 \times 24 \times 365$ ), but only  $1 \times 0.35 \times 24 \times 365 = 3,066$  MW·h, averaging to 0.35 MW. Unlike fuelled generating plants, the capacity factor is limited by the inherent properties of wind. Capacity factors of other types of power plant are based mostly on fuel cost, with a small amount of downtime for maintenance [1].

In Figure 1-1, the global wind energy council (GWEC) published that over the past ten years, global wind power capacity has continued to grow at an average cumulative rate of over 30%, and 2008 was another record year with more than 27 GW of new installations, bringing the total up to over 120 GW. The United States passed Germany to become the number one market in wind power, and China's total capacity doubled for the fourth year in a row [3].

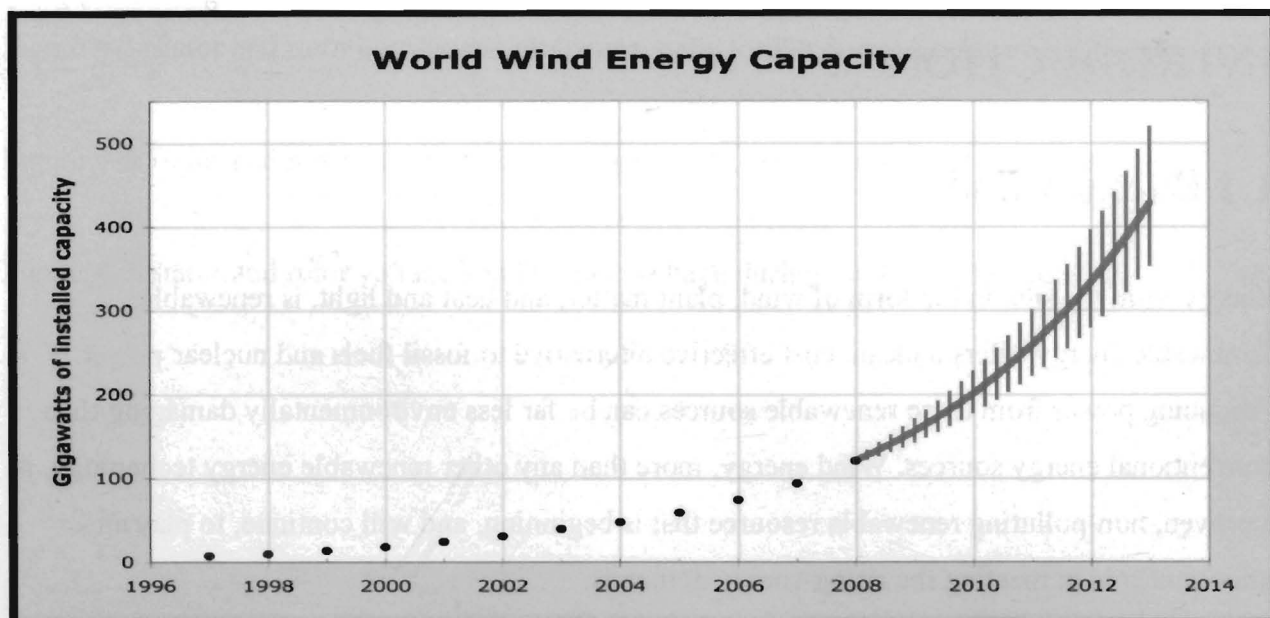


**Fig. 1-1 Worldwide wind energy capacity prediction, 2008 [3].**

Since wind speed is not constant, a wind farm's annual energy production is never as much as the sum of the generator nameplate ratings multiplied by the total hours in a year. The ratio of actual productivity in a year to this theoretical maximum is called the capacity factor. Typical capacity factors are 20–40%, with values at the upper end of the range in particularly favourable sites. For example, a 1 MW turbine with a capacity factor of 35% will not produce 8,760 MW·h in a year ( $1 \times 24 \times 365$ ), but only  $1 \times 0.35 \times 24 \times 365 = 3,066$  MW·h, averaging to 0.35 MW. Unlike fuelled generating plants, the capacity factor is limited by the inherent properties of wind. Capacity factors of other types of power plant are based mostly on fuel cost, with a small amount of downtime for maintenance [1].

In Figure 1-1, the global wind energy council (GWEC) published that over the past ten years, global wind power capacity has continued to grow at an average cumulative rate of over 30%, and 2008 was another record year with more than 27 GW of new installations, bringing the total up to over 120 GW. The United States passed Germany to become the number one market in wind power, and China's total capacity doubled for the fourth year in a row [3].

Across Canada, electricity generated from wind is powering almost one million homes and business in a clean, reliable and efficient manner. Canada ranks behind the United States and most European countries in wind energy installation. Despite a slower start, Canada is currently experiencing an annual 30% growth rate in wind energy development, a rate comparable to global development. With Canada's unparalleled wind resource, there are still opportunities to do more to maximize the economic, industrial development, and environmental benefits associated with wind energy for Canada. Canada's current installed capacity is 3,426 MW [5]. A year 2009 has been a record year for wind energy development in Canada with a new installed capacity of 950MW. Also, wind development operating in every province for first time ever in 2009.

The Canadian Wind Energy Association's goal is 10,000 MW of installed wind energy in Canada by the end of year 2010, enough to supply 5% of Canada's electricity needs. Denmark currently generates over 20% of its power from the wind, an attainable goal for Canada. If wind energy were to generate 20% of Canada's electricity, it would be the second largest source of electricity behind hydro and ahead of nuclear, natural gas and coal. Recent growth in Canada owes much to federal and provincial policy measures that have enabled or encouraged wind energy development. It is crucial that the government creates a level playing field for wind energy so that it can compete with conventional energy [2].

## **1.2 Wind Energy Conversion Systems**

In this section, properties of the wind, which are interest to DFIG, will be discussed. The wind distribution which is used to determine the output power will be presented. Finally, the aerodynamic conversion system will be analyzed with mathematical formulation.

Wind Energy Conversion Systems (WECS) convert the energy in moving air (the wind) to electrical energy. The basic idea is quite simple and has been around for centuries: the wind strikes some sort of set of blades mounted on a shaft that is free to rotate. The wind hitting the blades generates a force that turns the shaft, and this rotational kinetic energy may then be used for any of a number of purposes (historically, things like pumping water, moving a saw, or turning grain-grinding stones, to name a few). In a WECS, the rotating shaft turns an electric generator that converts the rotational kinetic energy to electric energy.

The major components of a typical wind energy conversion system include a wind turbine, generator, interconnection apparatus and control systems. Wind turbines can be classified into the vertical axis type and the horizontal axis type. Most modern wind turbines use a horizontal axis configuration with two or three blades, operating either down-wind or up-wind. A wind turbine can be designed for a constant speed or variable speed operation. Variable speed wind turbines can produce 8% to 15% more energy output as compared to their constant speed counterparts, however, they necessitate power electronic converters to provide a fixed frequency and fixed voltage power to their loads [6].

Power developed by the wind machine is mainly affected by wind speed, area swept by the rotor, density of air, rotational speed of the machine, radius of the rotor, number of blades, and total blade area. It is also affected by lift and drag characteristics of the blade profile. Some of the available power in the wind is converted by the rotor blades to mechanical power acting on the rotor shaft of the wind turbine. For steady-state calculations of the mechanical power from a wind turbine, the so called  $C_p(\lambda, \beta)$ -curve can be used. The mechanical power  $P_{mech}$  can be determined as follows:

$$P_{mech} = \frac{1}{2} \rho A_r C_p(\lambda, \beta) \omega^3 \quad (1.1)$$

$$\lambda = \frac{\Omega_r r_r}{\omega} \quad (1.2)$$

Where  $C_p$  is the power coefficient,  $\beta$  is the pitch angle,  $\lambda$  is the tip speed ratio,  $\omega$  is the wind speed,  $\Omega_r$  is the rotor speed (on the low-speed side of the gearbox),  $r_r$  is the rotor-plane radius,  $\rho$  is the air density and  $A_r$  is the area swept by the rotor. In Fig. 1.2, an example of a  $C_p(\lambda, \beta)$  - curve and the shaft power as a function of the wind speed for rated rotor speed, i.e., a fixed-speed wind turbine, can be seen.

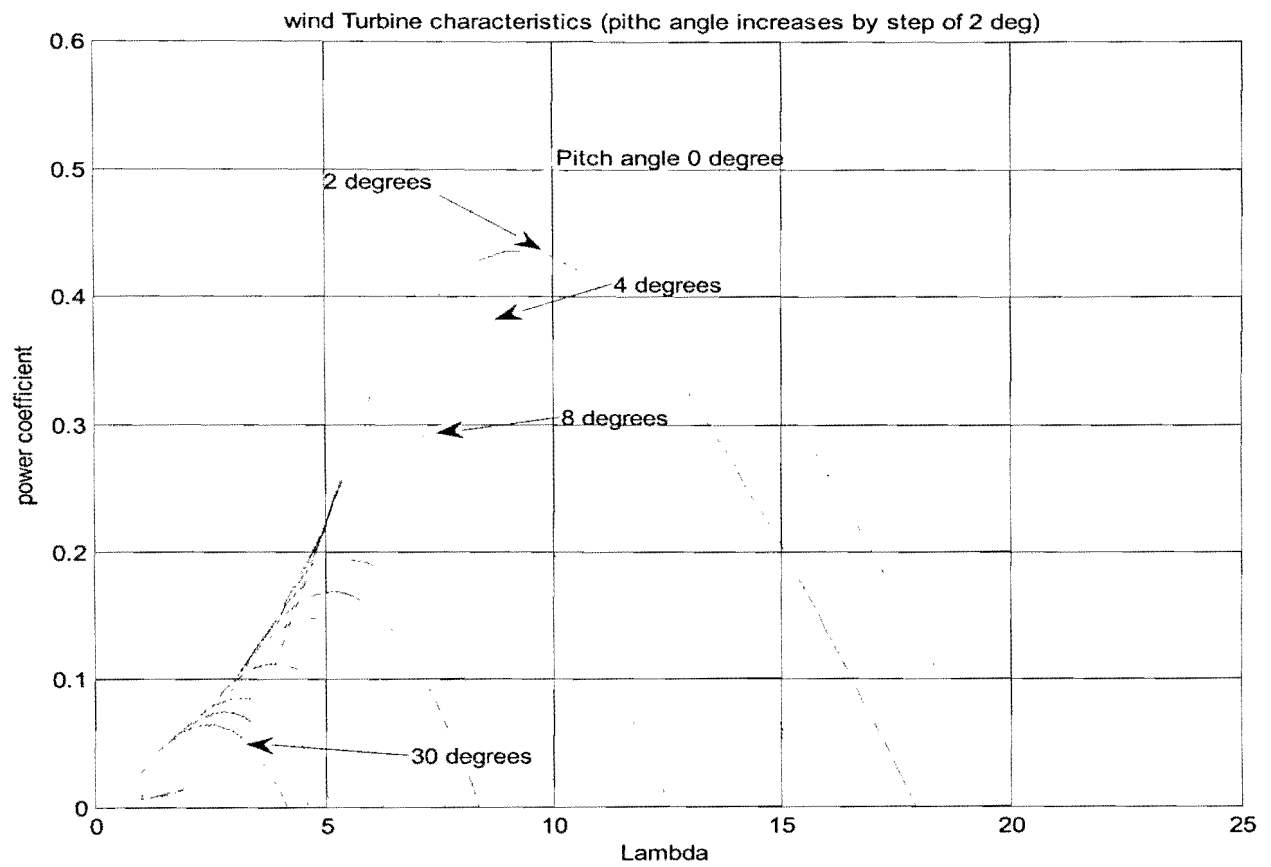


Fig. 1-2 the power coefficient,  $C_p$ , as a function of the tip speed ratio,  $\lambda$ .

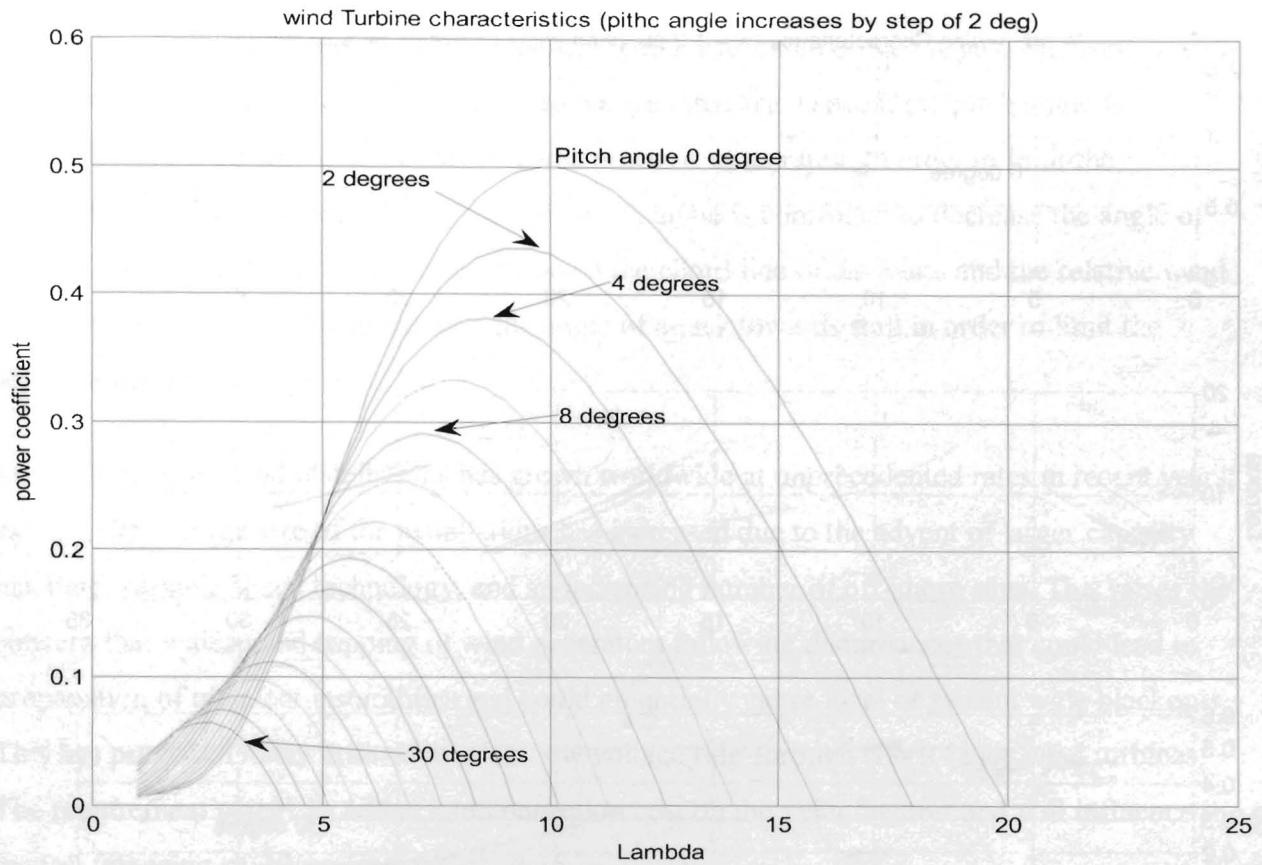
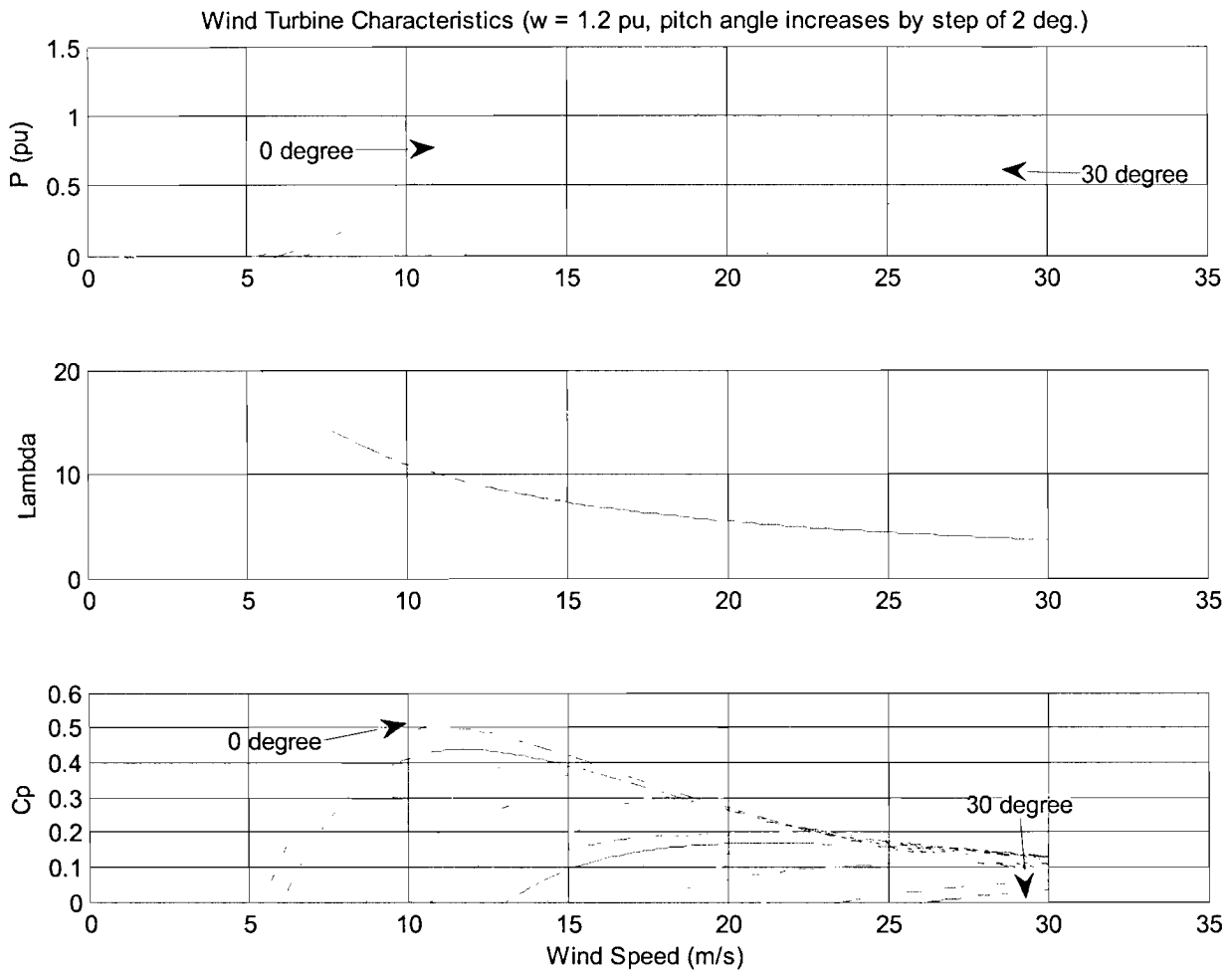


Fig. 1-2 the power coefficient,  $C_p$ , as a function of the tip speed ratio,  $\lambda$ .



**Fig. 1-3 The turbine power, the tip speed ratio  $\lambda$  and the  $C_p$ .**

The turbine  $C_p$  curves are displayed in Figure 1-2. The turbine power, the tip speed ratio  $\lambda$  and the  $C_p$  values are displayed in Figure 1-3 as function of wind speed. For a wind speed of 15 m/s, the turbine output power is 1 pu of its rated power, the pitch angle is  $8.7^\circ$  and the generator speed is 1.2 pu.

The speed of the wind is variable in nature; at high speed it's necessary to limit the input power to the wind turbines, i.e., aerodynamic power control. There are three major ways of performing the aerodynamic power control, stall, pitch, or active stall control. In stall control the blades are designed to stall in high speeds and no pitch mechanism is required. However, pitch control is the most common controlling method of aerodynamic power generated by a turbine rotor of



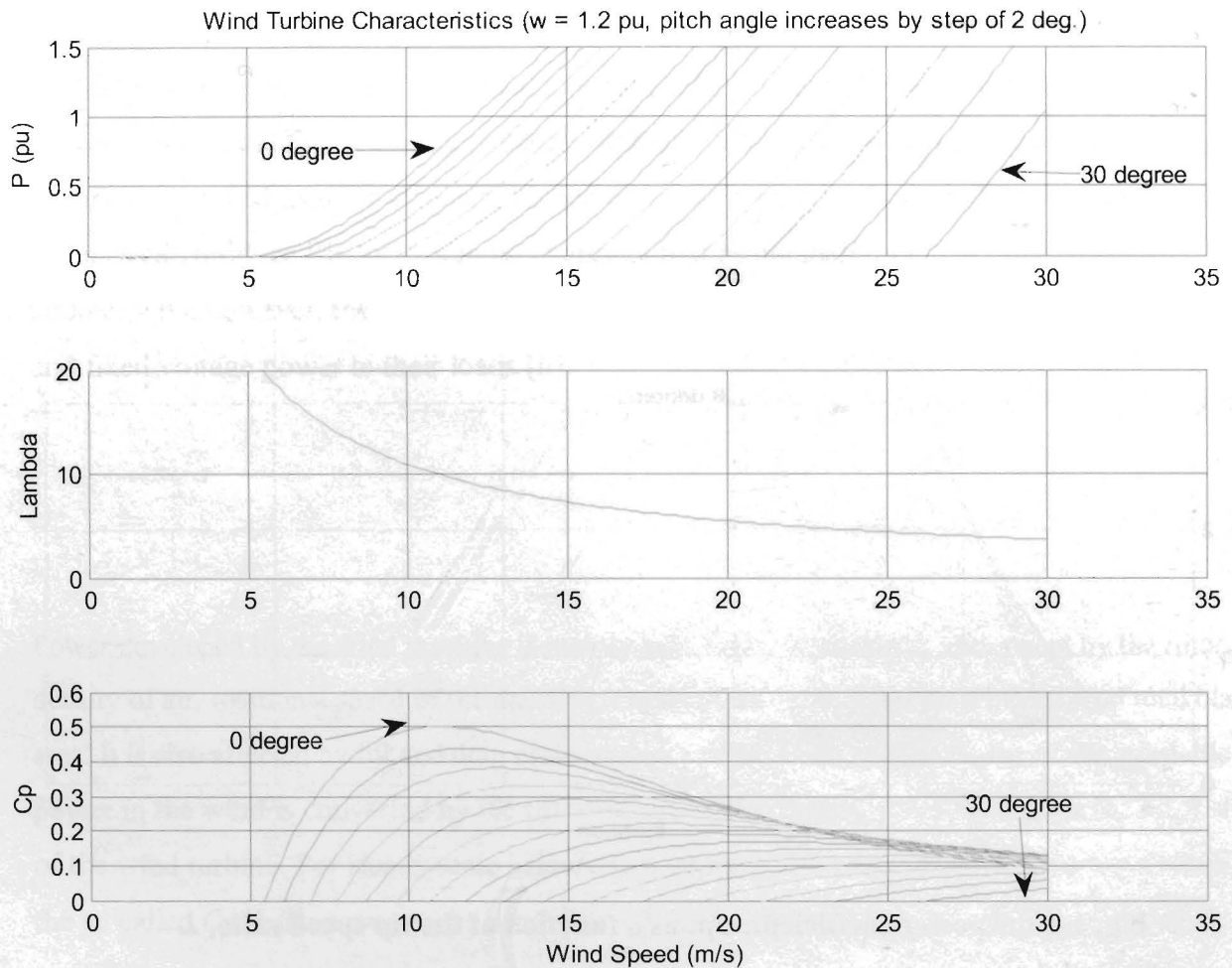


**Fig. 1-3 The turbine power, the tip speed ratio lambda and the  $C_p$ .**

The turbine  $C_p$  curves are displayed in Figure 1-2. The turbine power, the tip speed ratio lambda and the  $C_p$  values are displayed in Figure 1-3 as function of wind speed. For a wind speed of 15 m/s, the turbine output power is 1 pu of its rated power, the pitch angle is  $8.7^\circ$  and the generator speed is 1.2 pu.

The speed of the wind is variable in nature; at high speed it's necessary to limit the input power to the wind turbines, i.e., aerodynamic power control. There are three major ways of performing the aerodynamic power control, stall, pitch, or active stall control. In stall control the blades are designed to stall in high speeds and no pitch mechanism is required. However, pitch control is the most common controlling method of aerodynamic power generated by a turbine rotor of

modern and large wind turbines. Almost all variable-speed wind turbines use pitch control. Below the rated wind speed, the turbine should produce as much power as possible using a pitch angle that maximizes the energy capture. Above the rated wind speed, the pitch angle is controlled in such a way that the aerodynamic power is at its rated. In order to limit the aerodynamic power, at high wind speeds, the pitch angle is controlled to decrease the angle of attack. The angle of attack is the angle between the chord line of the blade and the relative wind direction. It's also possible to increase the angle of attack towards stall in order to limit the aerodynamic power [6].

As the number of wind installations has grown worldwide at unprecedented rates in recent years; as well, the average size of the installations has increased due to the advent of larger capacity machine, variable speed technology, and an increasing number of off-shore sites. This raises the concern that widespread tripping of wind generators following disturbances that could lead to propagation of transient instabilities and could potentially cause local or system wide blackouts. This has provoked many utilities to adopt low voltage ride-through (LVRT) for wind turbines. The requirement places an added interconnection cost on the manufacturer and will influence the overall financing of the project.

## **1.3 Low Voltage Ride Through (LVRT)**

According to the new grid codes, instead of disconnection, the wind generators have to support the network during the power disturbances in the network. Therefore, it is necessary to carry out accurate transient simulations in order to understand the impact of the power system disturbances on a wind turbine operation. In the recent years, the ride-through analysis of the DFIG wind turbine under network disturbance has become an intensively studied problem. Due to the random nature, faults imposed on the grid can occur anywhere within the connected system. Also, due to transmission line impedance the voltages dip could be seen at the stator windings. The voltage dip can cause excessive currents on the rotor windings by the magnetic coupling. As a fail-safe mechanism, the DFIG automatically disconnects from the grid protecting the internal power electronic converter from over currents as well as over voltage on the converter dc link [7].

Most of the DFIG wind generators transient studies have been focused on the voltage dip analyses due to symmetrical three phase network fault. These kinds of faults, however, are very seldom. Single and two-phase earth faults are more common. Moreover, two-phase faults are more demanding for a DFIG than symmetrical three-phase faults. Thus, more research about unsymmetrical fault ride-through performance is required. Most DFIG wind turbine models that are used in transient analyses represent the generator by means of a two-axis model with constant lumped parameters. A model of DFIG that takes into account the equivalent circuit parameter variation was presented in chapter 2. A significant part of the wind turbine model is the model of a frequency converter that supplies the rotor of the DFIG. The converter is found to be the most sensitive part of the wind turbine when subjected to a short-circuit fault in the grid. The control of a frequency converter is usually based on field oriented control but also, the modified direct torque control (DTC) could be used. The frequency converters are usually equipped with a rotor over current protection circuit that is commonly called crowbar. The crowbar protects the rotor-side frequency converter against the high rotor current transient that DFIG generates during the disturbance.

A Typical LVRT characteristic is more or less defined by a minimum voltage throughout the duration of the fault followed by a ramping up to nominal level as the voltage recovers. The width of this minimum is dictated by the length of time to normally clear a transmission level fault (10 to 20 cycles) which then ramps up to the normal operating range with a given slope [7, 8]. Although the width and magnitude of the minimum are dictated by protection technologies and the location and type of fault, the slope of the recovery likely depends on the strength of the interconnection and reactive power support, whereby stronger systems could afford a much steeper increase and thus minimize the ride-through requirements of the generators. The functional operation of LVRT is based on the comparison of the characteristic with that of the terminal voltage. Essentially, once the voltage dips outside of the normal operating range the control system then compares the recovery of the fault with that of the minimum voltage level as given by the LVRT characteristic. As shown in Fig. 1-4, in the case in which the voltage falls below that of the LVRT characteristic, the generator may trip, however, anywhere above the minimum, the generator must remain connected and support the grid [7].

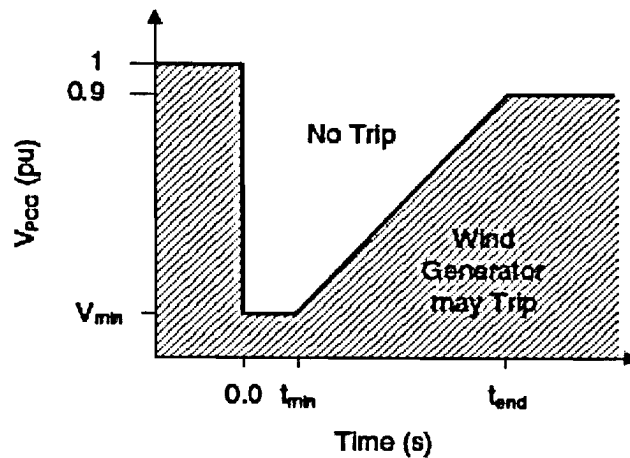


Fig. 1-4 Typical low ride- through voltage characteristics.

Under fault conditions, there are two major problems for existing DFIG based wind energy system:

1. Over current for rotor side converter and over voltage on dc link
2. Reconnection to recovered grid may cause stability issue.

Without proper control scheme, DFIG induces large currents on the rotor side as the excitation current is low during faults. The generator flux is not maintained when the stator voltage drops or negative rotating flux may appear if the system is severely unbalanced.

It's desirable to regulate the terminal voltage (or reactive power) in order to achieve voltage stability and maintain a smooth voltage profile at the point of interconnection [11]

Following fault recovery, the grid voltage increases to approximately 95% of the rated value, however, the grid is still considered to be very weak. An attempt to reconnect the WECS under this condition can make the system unstable as the WECS being reconnected it pulls the grid voltage low due to reactive power. In practice, the WECS do not connect to the grid immediately after fault recovery. In general, reconnection only occurs once it has been determined the grid is stable enough.

Conventionally, the control algorithm integrated to the wind turbine would have to be modified to incorporate fault detection and monitoring. In concurrence to the software, external hardware equipped to handle the fault operation under reduced supply voltage must be appropriately chosen for the application. The two most hardware solutions to solve the LVRT problem that have been researched and considered include: (i) power converter with UPS, in this method the UPS behaves as a source or a sink to allow the bidirectional power flow depending on the operation of the generator; (ii) active crowbar, power resistors are connected to the rotor windings and controlled to turn on absorbing excessive rotor energy [8]. The latter method is considered for this project and will be discussed further in chapter 4. The summaries of additional LVRT alternatives are shown in table 1-1. These techniques are all applicable and practical to overcome the LVRT challenge however the implementation cost per kilowatt hour is a determinant factor.

**Table 1-1 Summary of LVRT Methods [reference]**

LVRT Technology	Ride – Through duration
Additional Capacitors	0.1 seconds
Boost Converter	5 seconds
Battery Backup	5 seconds
Super Capacitors	5 seconds
Active Crowbar	0.3 seconds

The fault ride-through and grid support capabilities of the DFIG addresses primarily the design of DFIG wind turbine control with special focus on power converter protection and voltage control issues.

## 1.4 Motivation

DFIG has recently received much attention as one of preferred technology for wind power generation. Compared to a full rated converter system, the use of DFIG in a wind turbine offers many advantages, such as reduction of inverter cost, the potential to control torque and a slight increase in efficiency of wind energy extraction. However, the rotor power converter as a vulnerable part of the DFIG power converter, which has a restricted over-current limit, needs special attention especially during faults in the grid. When faults occur and cause voltage dips, subsequently the current flowing through the power converter may be very high (over-current). During this situation, it is common to block the converter to avoid any risk of damage, and then to disconnect the generator from the grid. However, the increasing trend of connecting high penetrations of wind farms to transmission networks has resulted in the transmission system operators revising their grid codes for the connection of large MW capacity wind farms. Therefore, it's required for WECS to remain connected to the grid during grid network disturbance. Reliable protection schemes and fault detection mechanisms are of great importance to meet the new grid requirement.

Motivated by the reasons above, this project provides a study of the dynamics of the grid connected wind turbine with DFIG. The project also proposes alternative detection scheme for the active crowbar operation. The implementation of the active crowbar with integrated fault detection depends only on the stator side voltage and DC link voltage. The difference between the proposed system and the traditional active crowbar is the rotor current sensors. In this project alternative solutions where the internal control of the wind turbine remain unchanged, and no additional current sensors necessary inside the DFIG, is investigated.

As a project case study, the behaviour of a 9-MW wind farm consisting of six 1.5 MW wind turbines connected to a 25-kV distribution system exports power to a 120-kV grid through a 30-km, 25-kV feeder under various transmission faults is investigated. Also the normal operation of the same wind farm is studied to observe the system response of DFIG. The DC link voltage of the DFIG is also monitored. The selected Wind turbine uses a doubly-fed induction generator

(DFIG) consisting of a wound rotor induction generator and an AC/DC/AC IGBT-based PWM converter. The main purpose of this project is the analysis of the DFIG for a WECS application both during steady-state operation and transient operation. In order to analyze the DFIG during transient operation both the control and the modeling of the system is of importance. Hence, the control and the modeling are also important parts of the project with the main focus on the Low voltage Ride-Through capability of DFIG based WECS.

## 1.5 Report Outline

In Chapter 1, the background of the wind energy system, wind energy conversion system and motivation of this project are presented. Chapter 1 also introduces the low voltage ride through capability of DFIG and grid connection codes. The report is organized to provide in depth information about the research done on the DFIG wind energy system, active crowbar and fault detection methods in the subsequent chapters.

Chapter 2 gives the theoretical explanation of the DFIG from the stator reference frame using the mathematical model and equivalent circuit analysis. The rotor side control scheme is discussed with vector control method.

Chapter 3 provides the DFIG response to different types of fault in the grid during disturbances. The behaviour of the DFIG is analyzed under variable wind conditions and when faults are introduced in to the network.

Chapter 4 presents the implementation and strategy of fault detection method and recommended protection scheme. Active crowbar protection is integrated to DFIG using Matlab/Simulink. System recovery is explained and simulation results verify the theory and the proposed protection technique.

The last chapter provides an overview of the research undertaking, briefly and summarizes the development of the active crow bar and DFIG generators for WECS. Finally, further research recommendation is discussed.



## CHAPTER 2

### MODEL AND OPERATING PRINCIPLE OF DFIG

In order to investigate the impacts of these doubly fed induction generators installations on the operation and control of the power system, accurate models are required. The doubly fed induction generator can supply power at constant voltage and constant frequency while the rotor speed varies. This makes it suitable for variable speed wind energy applications. Additionally, when a back-to-back converter is used in the rotor circuit, the speed range can be extended above synchronous speed and power can be generated both from the stator and the rotor. An advantage of this type of DFIG drive is that the rotor converter need only be rated for a fraction of the total output power, the fraction depending on the allowable sub- and super-synchronous speed range.

The rotor side converter (RSC) usually provides active and reactive power control of the machine while the grid-side converter (GSC) keeps the voltage of the DC-link constant. The additional freedom of reactive power generation by the GSC is not mostly used; the rotor side converters are used. However, within the available current capacity the GSC can be controlled to participate in reactive power generation in steady state as well as during low voltage periods. The GSC can supply the required reactive current very quickly while the RSC passes the current through the machine resulting in a delay. Both converters can be temporarily overloaded, so the DFIG is able to provide a considerable contribution to grid voltage support during short circuit periods. In this chapter the introduction of DFIG, AC/DC/AC converter control and finally the SIMULINK/MATLAB simulation for grid connected Doubly Fed Induction Generator is presented.

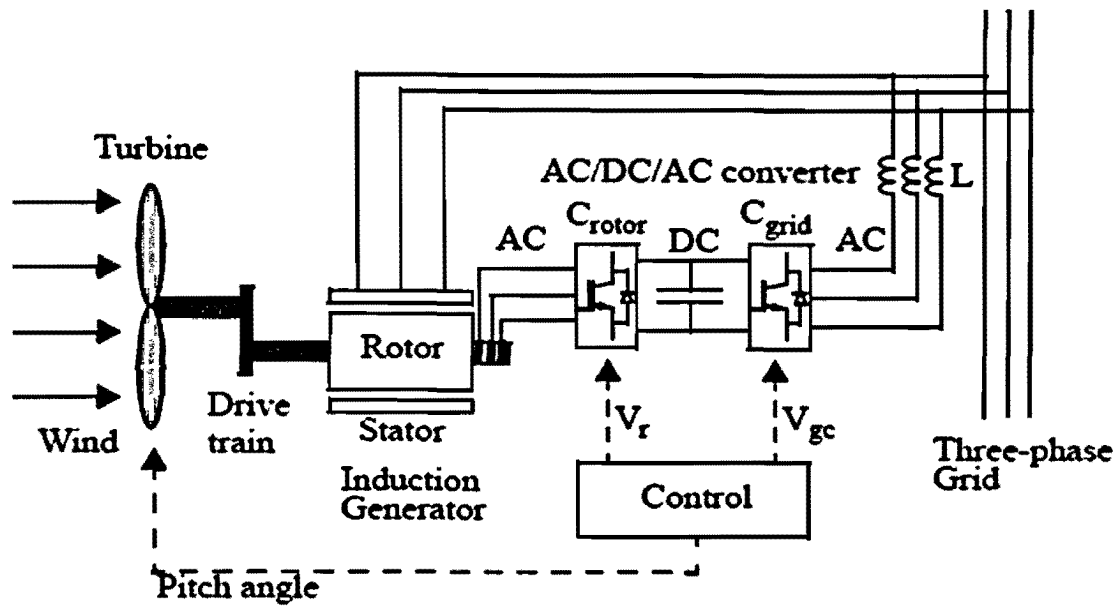


Fig. 2-1 General operating model of DFIG with converters.

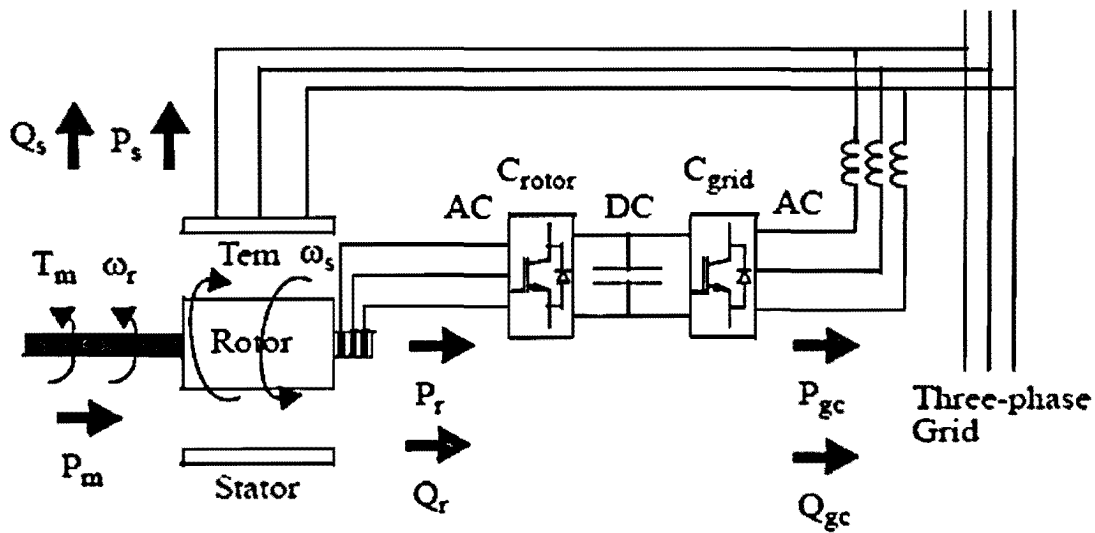


Fig. 2-2 Power flow diagram of DFIG.

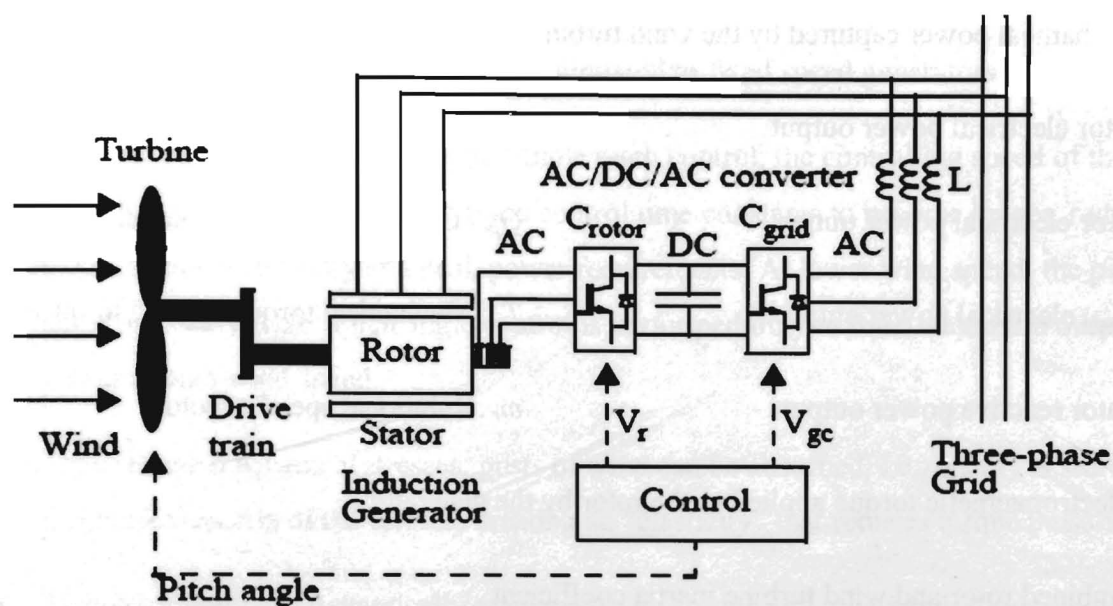


Fig. 2-1 General operating model of DFIG with converters.

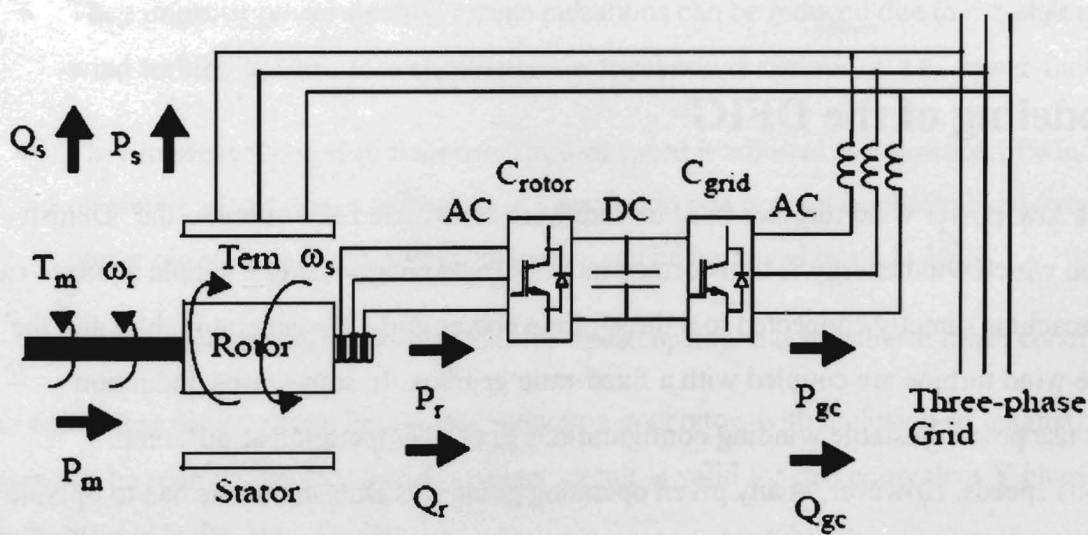


Fig. 2-2 Power flow diagram of DFIG.

The power flow parameters are:

$P_m$  - Mechanical power captured by the wind turbine and transmitted to the rotor

$P_s$  - Stator electrical power output

$Q_r$  - Rotor reactive power output

$P_r$  - Rotor electrical power output

$Q_{gc} - C_{grid}$  reactive power output

$P_{gc} - C_{grid}$  electrical power output

$T_m$  - Mechanical torque applied to rotor

$Q_s$  - Stator reactive power output

$\omega_r$  - Rotational speed of rotor

$T_{em}$  - Electromagnetic torque applied to the rotor by the generator

$J$  - Combined rotor and wind turbine inertia coefficient

$\omega_s$  - Rotational speed of the magnetic flux in the air-gap of the generator, this speed is named synchronous speed. It is proportional to the frequency of the grid voltage and to the number of generator poles.

## 2.1 Modeling of the DFIG

Most of the low-power wind turbines built to-date were constructed according to the “Danish concept”, in which wind energy is transformed into electrical energy using a simple squirrel-cage induction machine directly connected to a three-phase power grid. The generator shaft and the rotor of the wind turbine are coupled with a fixed-ratio gearbox. In some cases, induction generators use pole-adjustable winding configurations to enable operation at different synchronous speeds. However, at any given operating point, this Danish turbine has to operate at a constant speed. The construction and performance of fixed-speed wind turbines mainly depends on the characteristics of mechanical sub circuits, such as, pitch control time constants, main breaker maximum switching rate and etc. The response time of the mechanical circuits is may be in the range of tens of milliseconds. As a result, each time a gust of wind hits the turbine, a fast and strong variation of electrical output power can be observed. Due to these load variations, it requires a stiff power grid to enable stable operation and a sturdy mechanical design

to absorb high mechanical stresses. Overall, this construction strategy results in expensive mechanical construction, especially at high-rated power [10].

Key advantages of adjustable speed generator compared to fixed speed generators

- They are cost effective and provide simple pitch control; the controlling speed of the generator (frequency) allows the pitch control time constants to become longer, reducing pitch control complexity and peak power requirements. At lower wind speed, the pitch angle is usually fixed. Pitch angle control is performed only to limit maximum output power at high wind speed.
- They reduce mechanical stresses; gusts of wind can be absorbed, i.e., energy is stored in mechanical inertia of the turbine, creating an “elasticity” that reduces torque pulsations.
- They have ability to dynamically compensate for torque and power pulsations caused by back pressure of the tower. This back pressure causes noticeable torque pulsations at a rate equal to the turbine rotor speed times the number of rotor wings.
- They improve power quality; torque pulsations can be reduced due to the elasticity of the wind turbine system. This eliminates electrical power variations, i.e., fewer flickers.
- They improve the system frequency; turbine speed is adjusted as a function of wind speed to maximize output power. Operation at a maximum power point can be realized over a wide power range. As a result, energy efficiency can be improved by up to 10%.
- They reduce acoustic noise, because low speed operation is possible at lower conditions.

The equivalent circuit of the doubly-fed induction generator, with inclusion of magnetizing losses can be seen in Fig. 2.3. The equivalent circuit is valid for one equivalent Y phase and for steady-state calculations

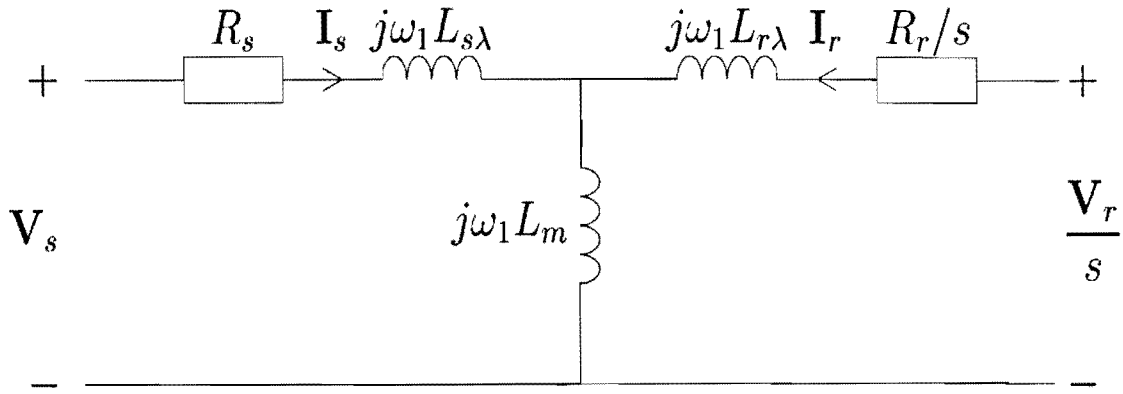


**Fig. 2-3 Equivalent circuit of Doubly Fed Induction Generator.**

In the case that the DFIG is delta connected the machine can still be represented by this equivalent Y representation. In this section the  $j\omega$ - method is adopted for calculations. Note, that if the rotor voltage,  $V_r$ , in Fig. 2.3, is short circuited the equivalent circuit for the DFIG becomes the ordinary equivalent circuit for a cage-bar induction machine. Applying Kirchhoff's voltage law to the circuit in Fig. 2.3 yields [6, 10]

$$V_s = R_s I_s + j\omega_1 L_{s\lambda} I_s + j\omega_1 L_m (I_s + I_r) \quad (2.1)$$

$$\frac{V_r}{s} = \frac{R_r}{s} I_r + j\omega_1 L_{r\lambda} I_r + j\omega_1 L_m (I_s + I_r) \quad (2.2)$$

The following notations are used;

$V_s$  stator voltage;

$R_s$  stator resistance;

$V_r$  rotor voltage;

$R_r$  rotor resistance;

$I_s$  stator current;

$I_r$  rotor current;

$L_{s\lambda}$  stator leakage inductance

$L_{r\lambda}$  rotor leakage inductance;

$\omega_1$  stator frequency;

$L_m$  magnetizing inductance;

$L_m$  magnetizing inductance;

$S$  slip.

The slip,  $S$ , equals

$$S = \frac{\omega_1 - \omega_r}{\omega_1} = \frac{\omega_2}{\omega_1} \quad (2.3)$$

Where  $\omega_r$  is the rotor speed and  $\omega_2$  is the slip frequency. Moreover, if the air gap flux, stator flux and rotor flux are defined as

$$\psi_m = L_m (I_s + I_r) \quad (2.4)$$

$$\psi_s = L_{s\lambda} I_s + L_m (I_s + I_r) = L_{s\lambda} I_s + \psi_m \quad (2.5)$$

$$\psi_r = L_{r\lambda} I_r + L_m (I_s + I_r) = L_{r\lambda} I_r + \psi_m \quad (2.6)$$

Equations (2.1)-(2.3) that describe the equivalent circuit can be rewritten as

$$V_s = R_s i_s + j\omega_1 \psi_s \quad (2.7)$$

$$\frac{V_r}{s} = \frac{R_r}{s} I_r + j\omega_1 \psi_r \quad (2.8)$$

The resistive losses of the induction generator are given by;

$$P_{loss} = 3 (R_s / I_s)^2 + R_r / I_r)^2 \quad (2.9)$$

And the electro-mechanical torque,  $T_e$ , can be expressed as

$$T_e = 3n_p I_m [\psi_m i_r^*] = 3n_p I_m [\psi_r I_s^*] \quad (2.10)$$

Where  $n_p$  is the number of pole pairs

The power flow equations of the DFIG system, stator apparent power  $S_s$  and rotor apparent power  $S_r$  can be found as

$$S_s = 3V_s i_s^* = 3 R_s |I_s|^2 + j3\omega_1 L_{s\lambda} |I_s|^2 + j3\omega_1 \psi_m I_s^* \quad (2.11)$$

$$S_r = 3V_r i_r^* = 3 R_r |I_r|^2 + j3\omega_1 L_{r\lambda} |I_r|^2 + j3\omega_1 \psi_m I_r^* \quad (2.12)$$

Rewriting equations (2.13) and (2.14)

$$S_s = 3 R_s |I_s|^2 + j3\omega_1 L_{s\lambda} |I_s|^2 + j3\omega_1 \frac{|\psi_m|^2}{L_m} - j3\omega_1 \psi_m I_r^* \quad (2.13)$$

$$S_r = 3 R_r |I_r|^2 + j3\omega_1 s L_{r\lambda} |I_r|^2 + j3\omega_1 s \psi_m I_r^* \quad (2.14)$$

Now the stator and rotor power can be determined as

$$P_s = \text{Re}[S_s] = 3 R_s |I_s|^2 + 3\omega_1 \text{Im}[\psi_m I_r^*] \approx 3\omega_1 \text{Im}[\psi_m I_r^*] \quad (2.15)$$

$$P_r = \text{Re}[S_r] = 3 R_r |I_r|^2 - 3\omega_1 s \text{Im}[\psi_m I_r^*] \approx -3\omega_1 s \text{Im}[\psi_m I_r^*] \quad (2.16)$$

The approximations are made because the resistive losses and the magnetizing losses have been neglected. Finally, the mechanical power produced by the DFIG can be determined from the above equations as the sum of the stator and rotor power.

$$P_{mec h} = 3\omega_1 \text{Im}[\psi_m I_r^*] - 3\omega_1 s \text{Im}[\psi_m I_r^*] = 3\omega_r \text{Im}[\psi_m I_r^*] \quad (2.17)$$

## 2.2 Rotor Side Converter

The aim of the rotor side converter is to control independently the active and reactive power. The active and reactive powers are not controlled directly, but by controlling the impressed rotor current. The rotor side converter operates in a stator flux  $d$ - $q$  reference frame, where the rotor current is split into a parallel and orthogonal component to the stator flux, respectively. A very fast inner control loop regulates the active and the reactive component of the rotor current. The current set points are defined by the slower outer control loop regulating the active and reactive power. In order to decouple these two parameters, generator quantities are calculated using vector control technique in a synchronous reference frame fixed to the stator flux [10]. The controller provides set point values of the quadrature and direct axis component of the rotor current ( $i_{qr}$  and  $i_{dr}$ ). The control of active power is realized according to the control diagram as illustrated in Fig. 2-4 [10]

In normal operation the aim of the rotor side converter controller is to control active and reactive power independently. The reference active power is provided by a maximum power tracking depending on the actual generator speed, which assures operation with maximum aerodynamic efficiency. During normal operation the reference reactive power is usually set to zero. For high wind speeds the speed of the turbine is limited to its rated speed, which implies indirectly that the



power is limited to its rated value, too. This is realized by means of a speed controller interacting with the pitch mechanism. [10].

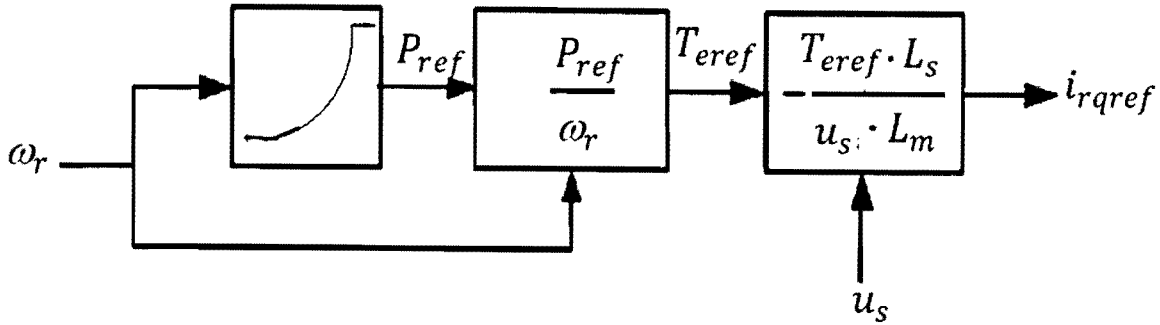
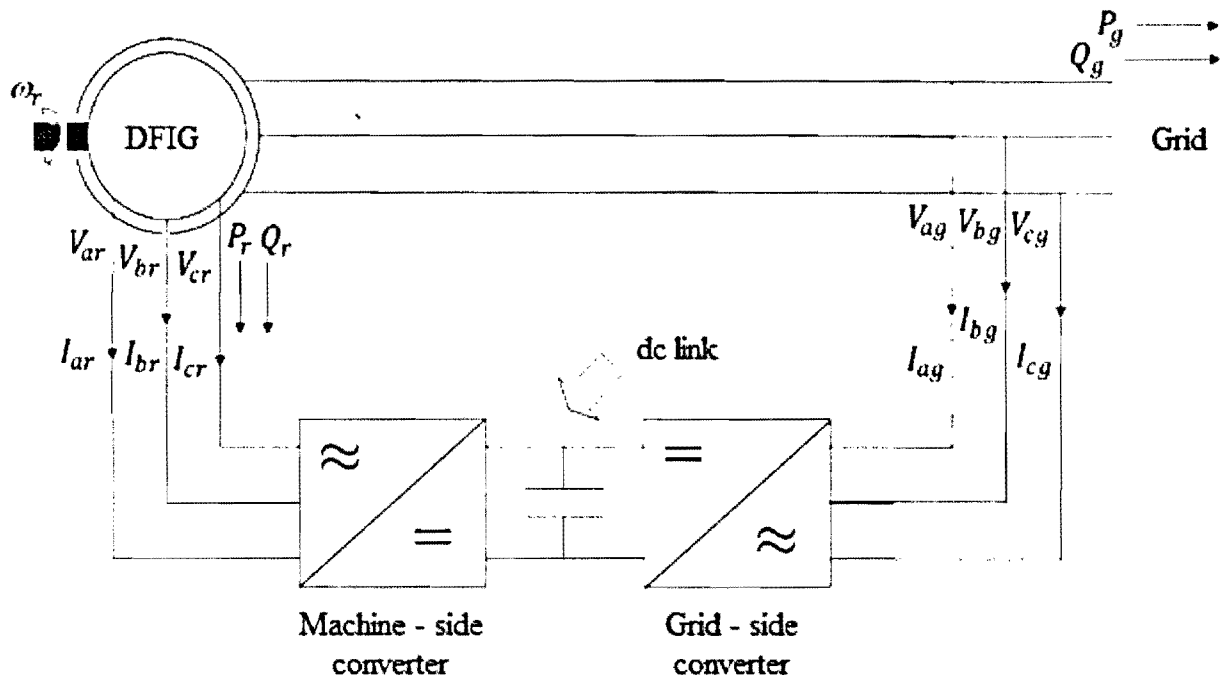


**Fig. 2-4 Rotor speed and active power control.**

It can be concluded that machine side converter behaves as a controlled current source providing power control through rotor current regulations.

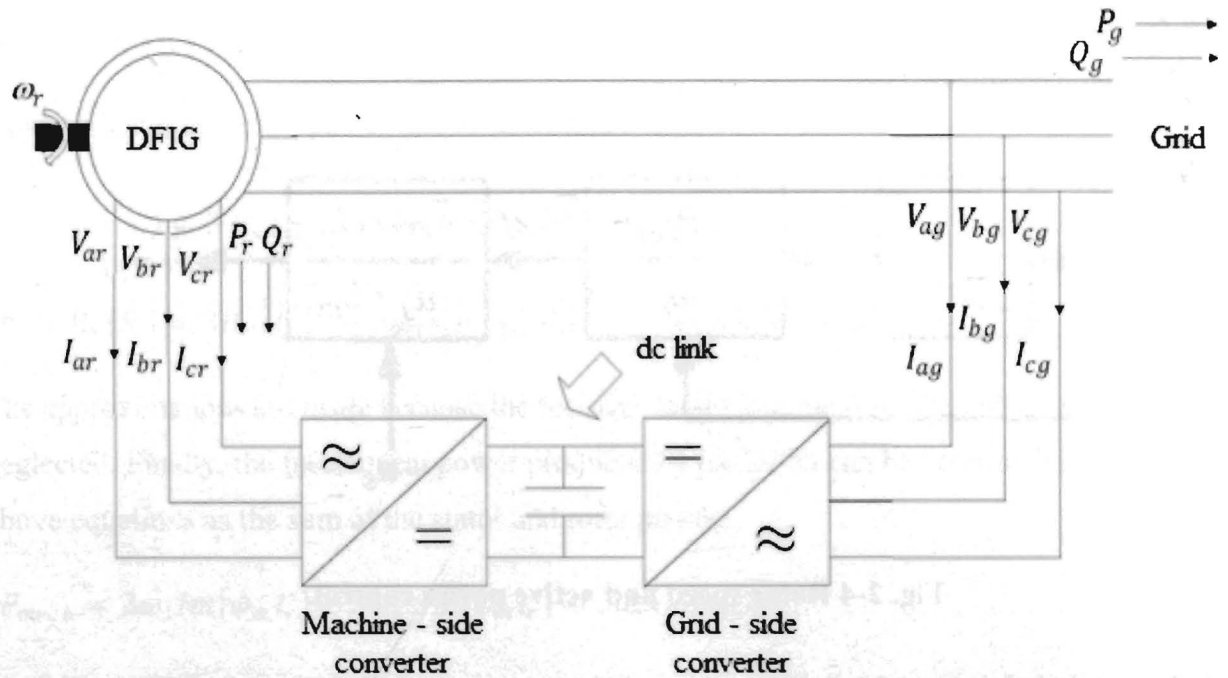
The implementation of the active and reactive power control is done by generating a reference current vector  $i_{dqr\_ref}$  which is proportional to the reactive power,  $Q_{ref}$  and the torque command,  $T_e$ .

The Field oriented control (also known as FOC) is the most popular among all Induction motor control mechanisms. This method is responsible for transforming the three phase time variant model, into a two coordinate (d and q co-ordinates) time invariant model. Fig. 2-5 shows the detailed block diagram of DFIG with the converters and the power flow variables according to the simulink model. The back-to-back converter consists of two converters, i.e., machine-side converters a dc-link capacitor placed, as energy storage, in order to the voltage variations (or ripple) in the dc-link voltage small. With the machine-side converter it is possible to control the torque or the speed of the DFIG and also the power factor at the stator terminals, while the main objective of the grid-side converter is to keep the dc-link voltage constant.



**2-5 Doubly fed induction generator with converters connected to a grid.**

The complexity of the mathematical model of induction motors makes it difficult to control the system with ease and accuracy. Using the FOC a structure that is similar to that of a DC machine control is commonly used. Two constants are required as reference inputs in the implementation of the FOC algorithm. These two reference inputs are the torque component (related to the q co-ordinate) and the flux component (related to the d co-ordinate). Since Field Orientated Control is only based on projections the control structure handles instantaneous electrical quantities. This makes the control to some extent accurate in every working operation (steady state and transient) and independent of the limited bandwidth mathematical model. The reactive power and voltage control is illustrated in Fig. 2-6



## 2-5 Doubly fed induction generator with converters connected to a grid.

The complexity of the mathematical model of induction motors makes it difficult to control the system with ease and accuracy. Using the FOC a structure that is similar to that of a DC machine control is commonly used. Two constants are required as reference inputs in the implementation of the FOC algorithm. These two reference inputs are the torque component (related to the q co-ordinate) and the flux component (related to the d co-ordinate). Since Field Orientated Control is only based on projections the control structure handles instantaneous electrical quantities. This makes the control to some extent accurate in every working operation (steady state and transient) and independent of the limited bandwidth mathematical model. The reactive power and voltage control is illustrated in Fig. 2-6

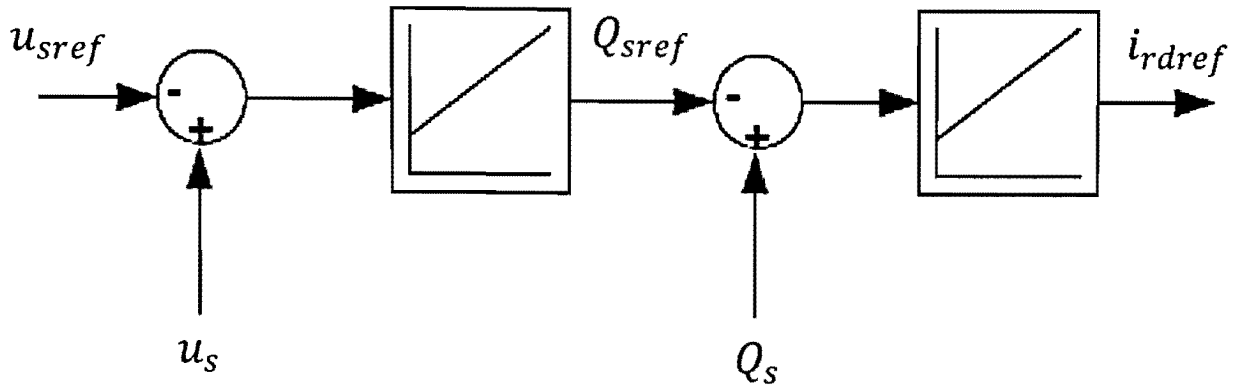


Fig. 2-6 Reactive power and voltage control diagram.

## 2.3 Grid Side Converter

The aim of the control of the grid side converter is to maintain the dc-link capacitor voltage in a set value regardless of the magnitude and the direction of the rotor power and to guarantee a converter operation with unity power factor (zero reactive power). This means that the grid side converter exchanges with the grid only active power, and therefore the transmission of reactive power from DFIG to the grid is done only through the stator. The dc-voltage and the reactive power are controlled indirectly by controlling the grid side converter current [11]. The aim of the grid side converter controller for normal operation is to maintain the DC-link capacitor voltage and to guarantee a converter operation with unity power factor. Detailed explanations about the control concept of the DFIG wind turbine concept for normal operation conditions can be found in [12].

In contrast to the rotor side converter the grid side converter can stay active during grid faults, when the rotor side converter is blocked by the crowbar. The grid side converter can then be used as a STATCOM and contribute supplementary to reactive power supply.

## 2.4 DFIG Normal Operation Analysis

The control scheme of the normal operation DFIG based system is illustrated using a 9 MW wind farm consisting of six 1.5 MW wind turbines connected to a 25 kV distribution system exports power to a 120 kV grid through a 30 km, 25 kV feeder. Wind turbines using a doubly-fed induction generator (DFIG) consist of a wound rotor induction generator and an AC/DC/AC IGBT-based PWM converter. The stator winding is connected directly to the 60 Hz grid while the rotor is fed at variable frequency through the AC/DC/AC converter. The DFIG technology allows extracting maximum energy from the wind for low wind speeds by optimizing the turbine speed, while minimizing mechanical stresses on the turbine during gusts of wind. [12,13]

The DFIG is modelled using a wound rotor asynchronous generator in the stationary frame where the stator and rotor winding are excited separately. The generator is a three pole-pairs machine whose rotor is connected in Y-connection to an internal neutral point. The generator parameters are listed in Table 2-1.

Table 2-1 DFIG System and model parameters

Nominal power [MVA]	1.5
Nominal voltage [Vrms]	575
Nominal frequency [Hz]	60
Stator resistance [pu]	0.00706
Rotor resistance, $R_s$ [pu]	0.005
Magnetization inductance, $L_m$ [pu]	2.9
Stator leakage inductance, $L_s$ [pu]	0.171
Rotor leakage inductance, $L_r$ [pu]	0.156
DC link voltage, $V_{dc}$ [V]	1200
Inertia constant [s]	5.04
Friction factor [pu]	0.01
DC link capacitor [ $\mu$ F]	10,000
Nominal line-to-line voltage [ $V_{LL}$ , RMS]	575

Nominal output frequency [Hz]	60
-------------------------------	----

The control system of the DFIG subsystem is explained in previous sections. The stator voltage, stator current, rotor current, rotor speed and DC link voltage are sensed and fed to controllers. The wind turbine information are utilised by the controller. The mechanical torque data is extracted and manipulated in the torque regulator producing the torque command [8, 9].

Three main controllers perform independent functions in order to obtain the desired output:

1. Speed controller uses the MPPT curve to build the reference speed and turbine output power. The torque command is extracted by estimating that stator speed.
2. Reactive power regulator is a closed loop with feedback from the collector bus of power quality control.
3. Current regulator regulates the rotor current with respect to the reference value. The reference values are generated from torque command and the relative power regulator.

The normal operation of DFIG is simulated and the results are presented in Figure 2.9

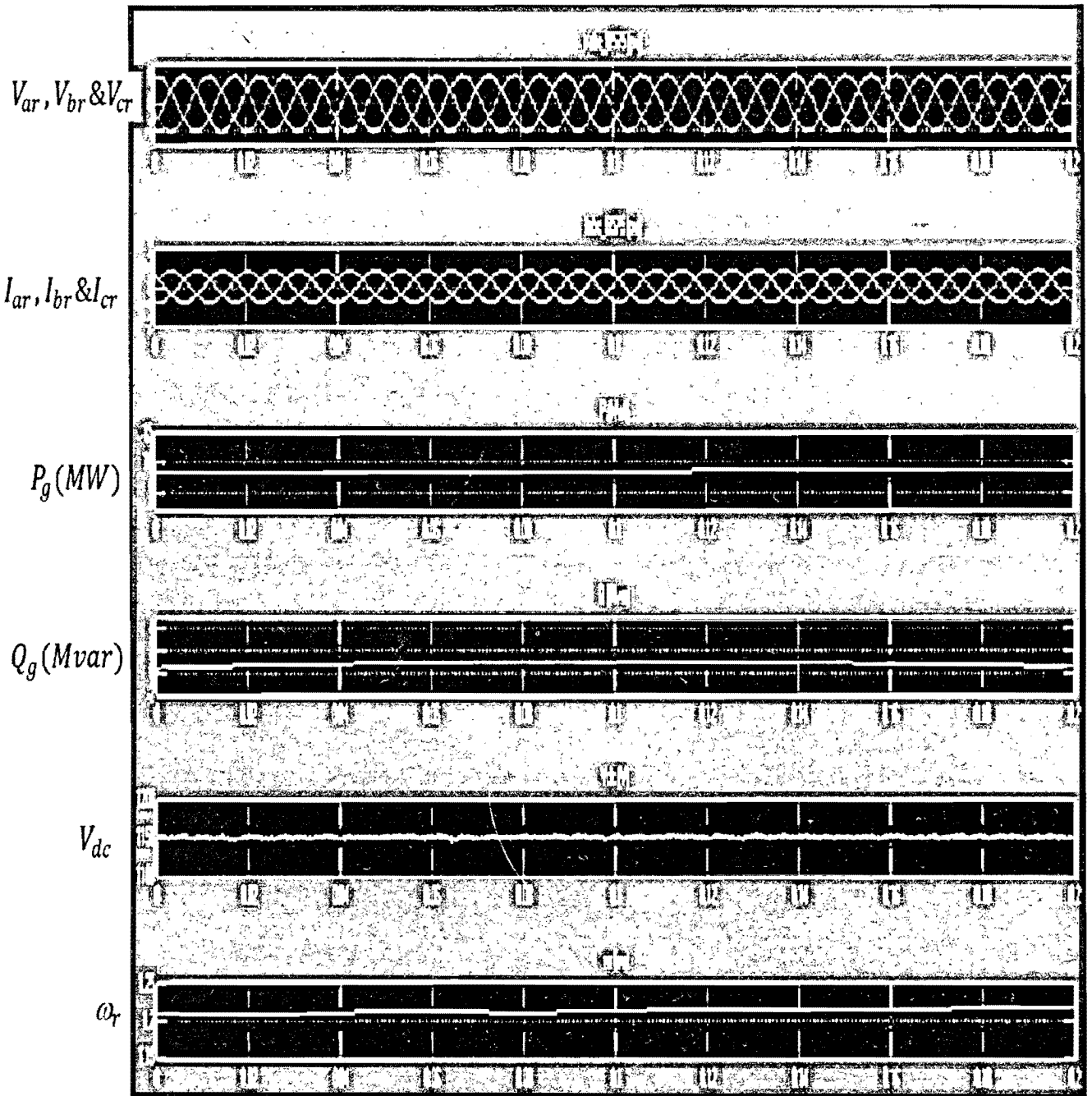
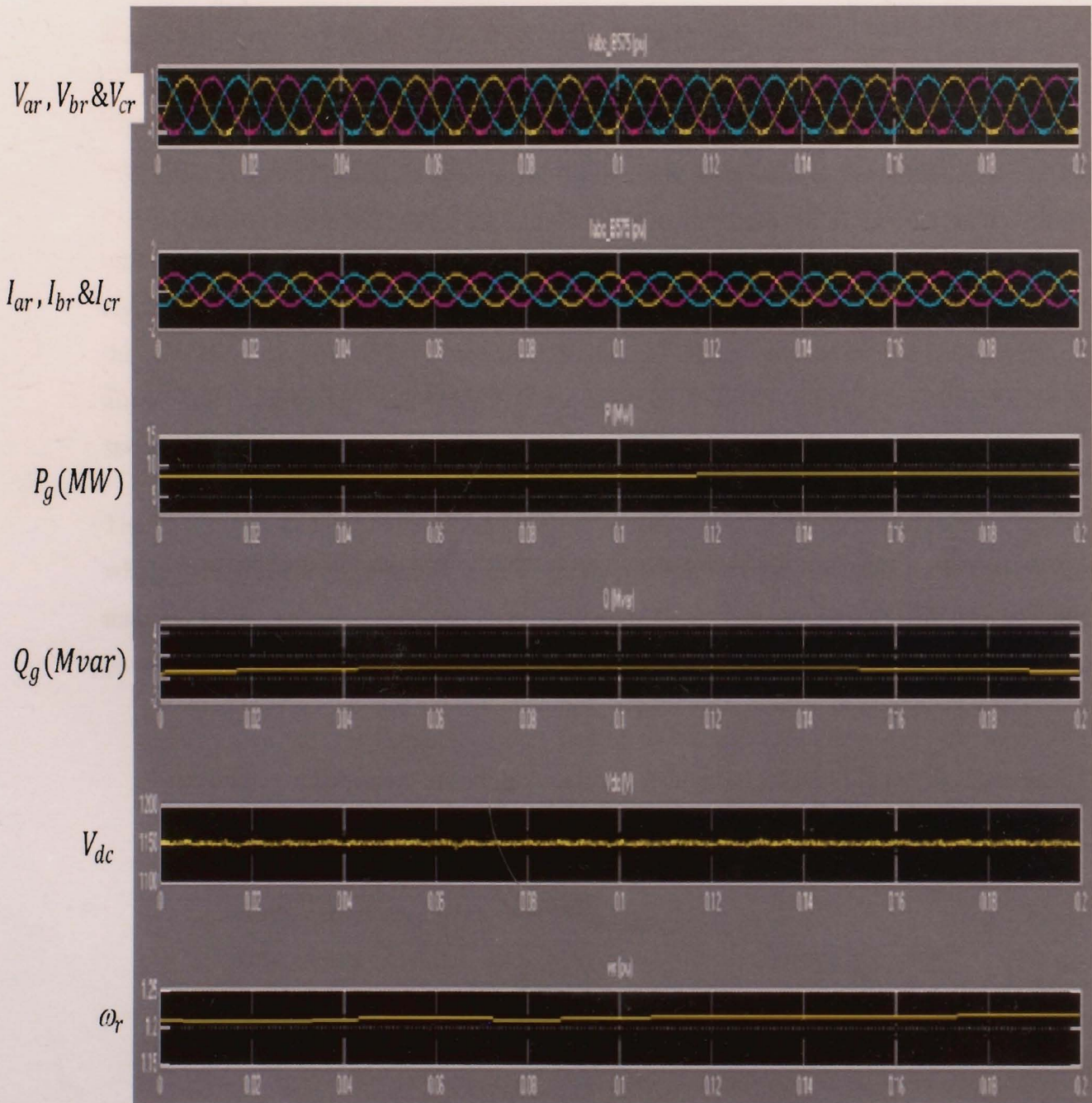


Fig. 2-8 DFIG during normal operation.

From Fig 2-9, the generator is operating in super-synchronous mode where the rotor is operating above the synchronous speed and the DC link voltage is maintained at the rated value (1150V). The rotor current reaches its pick value nearly 1.0 pu at start, and then slightly lower when it approaches the steady state. During the simulation the wind speed is maintained constant at 15 m/s. The control system uses a torque controller in order to maintain the speed at below the rated





**Fig. 2-8 DFIG during normal operation.**

From Fig 2-9, the generator is operating in super-synchronous mode where the rotor is operating above the synchronous speed and the DC link voltage is maintained at the rated value (1150V). The rotor current reaches its pick value nearly 1.0 pu at start, and then slightly lower when it approaches the steady state. During the simulation the wind speed is maintained constant at 15 m/s. The control system uses a torque controller in order to maintain the speed at below the rated



speed. The reactive power produced by the wind turbine is regulated at 0 Mvar with a slight fluctuation as seen in the plot. The DFIG wind farm produces 9 MW at the corresponding turbine speed of 1.2 pu of generator synchronous speed. Overall, the control performance of the DFIG is very good in normal conditions allowing active and reactive power changes in the range of few milliseconds.

## 2.5 Summary

A 9-MW wind farm consisting of six 1.5 MW wind turbines connected to a 25-kV distribution system exports power to a 120-kV grid through a 30-km, 25-kV feeder is studied for normal operation of DFIG. The DC link voltage of the DFIG is also monitored. The Wind turbine uses a doubly-fed induction generator (DFIG) consisting of a wound rotor induction generator and an AC/DC/AC IGBT-based PWM converter. The stator winding of the DFIG is connected directly to the 50 Hz grid while the rotor is fed at variable frequency through the AC/DC/AC converter. The DFIG technology allows extracting maximum energy from the wind for low wind speeds by optimizing the turbine speed, while minimizing mechanical stresses. The result from simulation of the WECS (wind energy conversion systems) under normal operation verifies the theoretical operation and chosen control scheme of DFIG. The flux oriented (FOC) control scheme is chosen for the machine side converter, the stator active and reactive power control offers better system stability while decoupling the  $d$ - $q$  components of the rotor current and controlling each power term separately. DFIG control can, within limits, hold their power constant in spite of fluctuating wind, storing thus temporarily the rapid fluctuations in power as kinetic energy.

## CHAPTER 3

### FAULT ANALYSIS OF DFIG

Due to the double fed induction generator's (DFIG) advantage of controlling active and reactive power independently and partial power converter, DFIG is becoming a popular type of wind power generation system. Nowadays, the grid code demands that the wind power generator possesses the ability of riding through the grid voltage sags, only when the grid voltage drops below the specific curve, the wind turbine is allowed to disconnect. DFIG wind power system has serious problems with the corresponding voltage sag as its partly power converter: depending on the depth and the conditions at the start of the sag, current, power and reactive power peaks may exceed rated values and may lead to a system shut down. [22]

In general these grid codes represent the fundamental guidelines for wind turbine manufacturers and wind farm planners. Basically, the North America, grid code follows their European counterpart categorising wind turbine capabilities as follows

- (i) Low voltage Ride-through (LVRT) requirement to keep wind turbines on the grid during faults by introducing new technologies.
- (ii) When tripping, wind turbines have to guarantee reconnection and continuation of power generation in the shortest possible time.
- (iii) The establishment of mechanisms for ascertaining and continuous monitoring of the fulfilment of grid requirements.
- (iv) Establishing intelligent system protection devices to ensure a minimum loss of wind power and to guarantee fast recovery of normal operation.

The new grid codes requirements includes voltage level, Total Harmonic Distortion (THD) levels in the point of common coupling (PCC) as well as the ride through capabilities during fault events in the grid. Also, the new wind turbines/farms should contribute to regulation if active and reactive power and thereby contribute to the frequency and voltage control [25].

One of the challenges of DFIG is that it does not handle faults in the manner of conventional generator during grid disturbances. Some of the critical problems that encounter DFIG under fault conditions are the following: (i) rotor over current which can cause the machine side converter to be damages or to be offline due to protection; (ii) DC link over-voltage which can lead to capacitor failure; (iii) temporary loss of control of the active and reactive power causing oscillations at the DFIG output; (iv) reactive power compensation during voltage imbalance. In order to avoid damage, WECS are tripped offline, separating the turbine from the grid. Thus, utilities are recognizing the need for WECS to withstand grid disturbances even if the voltage drops at the point of connection. The disturbances are classified as balanced or unbalanced. Based on the network configuration and WECS topology, the turbine may experience different situations at the turbine input terminals. The grid requires intelligent protection schemes to avoid voltage collapse and handle fault conditions in a shorter duration. Further analysis and the recommended method will be discussed in the next chapter.

In this chapter, short circuit faults are introduced in the simulation to study the response of DFIG. These faults are imposed along the transmission line and are categorised either as shorted phase(s) to ground or arching between phases. In the simulation the analysis of DFIG behaviour under each fault condition and undesirable fault response characteristics will be observed in the large peak currents at the initiation of the fault.

### **3.1 Double Fed Induction Generator during Fault**

Wind turbines based on DFIG have the stator windings connected directly to the grid, making the rotor winding susceptible to high currents induced during grid faults. The rotor windings are connected to the grid via a back-to-back converter, which is very sensitive to over-currents. The most common way to avoid high induced currents in the rotor side converter (RSC) is the use of a crowbar system. The crowbar system makes the DFIG behave in the same way as a conventional Squirrel Cage Induction Generator (SCIG) with higher rotor resistance expanding the critical rotor speed during the disconnection of the RSC from the rotor winding [22]. In the following sections the response of DFIG to various types of faults is analyzed and presented.

### 3.2 Three Phase Shorted to Ground

The balanced (or three phase) fault is the one when all three lines are shorted to ground. It is usually rare, but can happen. When a fault occurs it is important to isolate it by opening protective breakers. For a three phase symmetrical fault, at the instant of fault, all three voltages reach a value of  $V$

$$V_a = V_b = V_c = V \quad (15)$$

Addition of the three phase-currents should be zero

$$I_a + I_b + I_c = 0 \quad (16)$$

Another type of fault is Asymmetrical faults

1) Phase to phase faults (phase 'a' to phase 'b')

$$I_c = 0 \quad (17)$$

$$I_a + I_b = 0 \quad (18)$$

$$V_b = V_c = V \quad (19)$$

2) Single phase to ground faults (phase 'a' to ground)

$$V_a = 0 \quad (20)$$

$$I_b = I_c = 0 \quad (21)$$

The following simulation results illustrate the DFIG response during three phase fault in the transmission. The analysis was carried out in Matlab – Simulink simulation environment. The fixed simulation time-step was set to  $0.5e-7$  and forward Euler method was used.

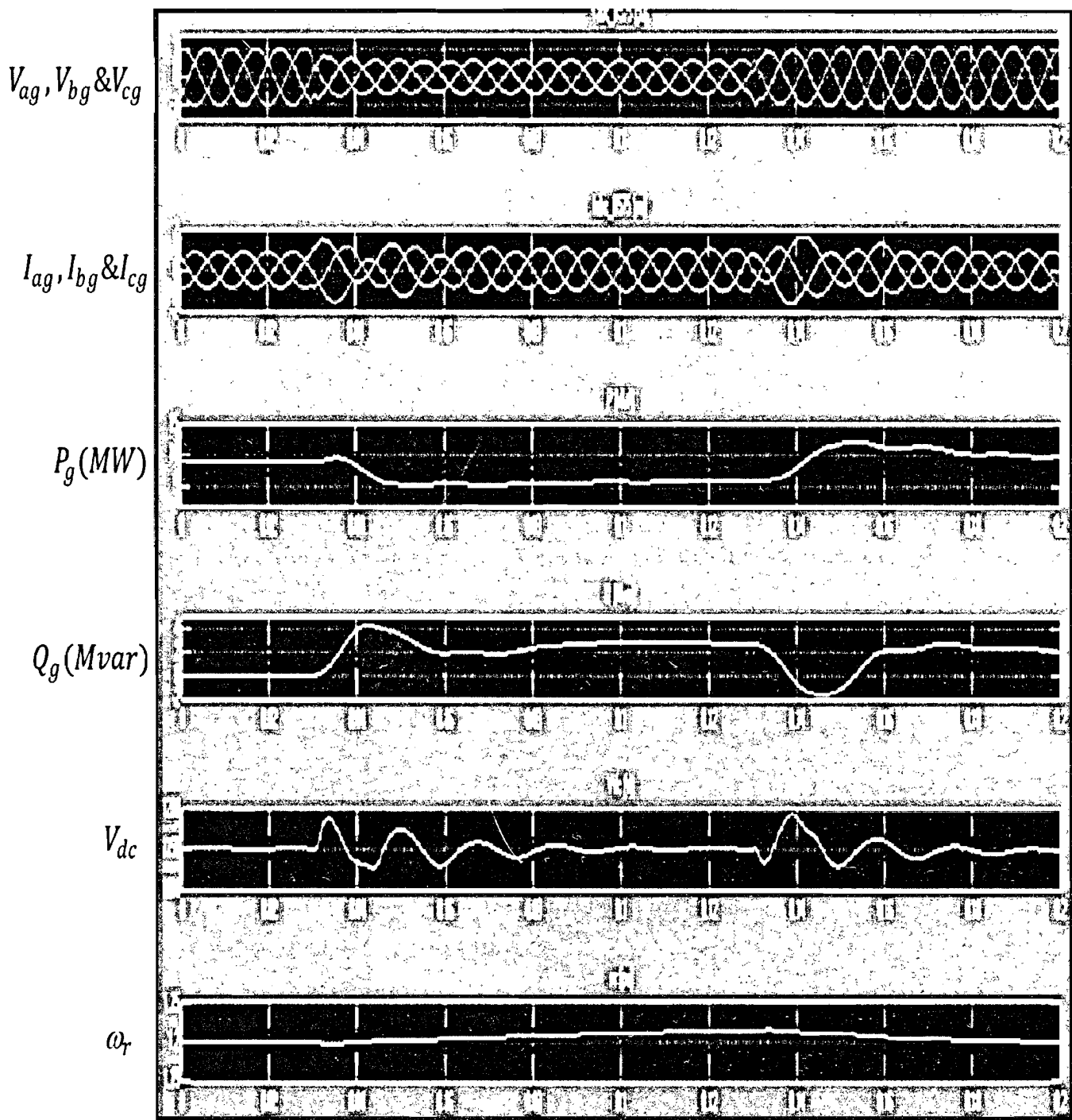
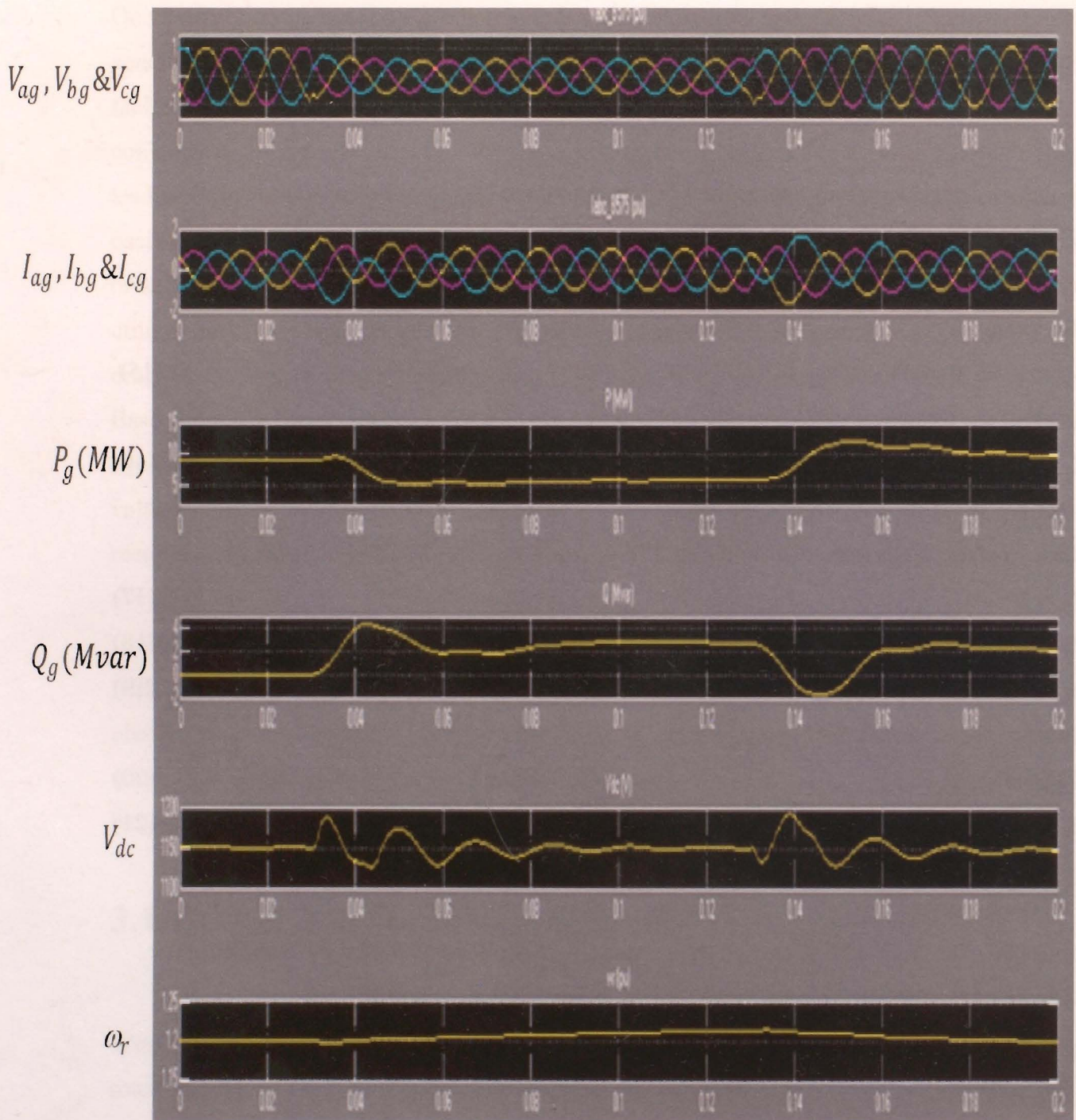


Fig. 3-1 DFIG during a voltage sag.

In Fig 3-1 the steady-state operation of the DFIG and its dynamic response to voltage sag resulting from a remote fault on the 120-kV system is plotted. The fault was introduced at  $t=0.03s$  and removed at approximately  $t=0.13s$ . Initially the DFIG wind farm produces to 9 MW.



**Fig. 3-1 DFIG during a voltage sag.**

In Fig 3-1 the steady-state operation of the DFIG and its dynamic response to voltage sag resulting from a remote fault on the 120-kV system is plotted. The fault was introduced at  $t=0.03s$  and removed at approximately  $t=0.13s$ . Initially the DFIG wind farm produces to 9 MW.

The corresponding turbine speed is 1.2 pu of generator synchronous speed. The DC voltage is regulated at 1150 V and reactive power is kept at 0 Mvar. At  $t=0.03$  s the positive-sequence voltage suddenly drops to 0.5 pu. causing an oscillation on the DC bus voltage and on the DFIG output power. During the voltage sag the control system tries to regulate DC voltage and reactive power at their set points (1150 V, 0 Mvar). The system recovers in 4 cycles at approximately  $t=0.13$ s.

Under normal operation, the DC link voltage has a steady value of approximately 1200V with some AC ripples. During fault, the capacitor voltage increases above its rated value to a peak of approximately 2000V, shown in Fig. 3-1. Also, the rotor current during fault is very high when compared with the rated value of 1pu. This can result in high stator voltage across DC link capacitor. Before the fault is applied, the active power output of the wind turbine is 0.2 pu while the reactive power output is kept constant at 0 pu. Approximately 100 ms after fault is cleared the terminal voltage is recovered (back to the steady state value) at 1 pu. This fast voltage recovery is due to the ability of DFIG to control the reactive power; damping control helps a quick recovery of DFIG after a fault on the grid.

### **3.3 Two-Phase Shorted**

A two phase fault is simulated in the same location as the three phase fault, where only two phases are shorted to ground. The simulation results are shown in the following figures. With unbalanced voltage, large rotor currents are induced in the rotor currents. This type of fault is not as severe as the three phase fault, but it can still cause an interruption to the power system and damage to the devices.



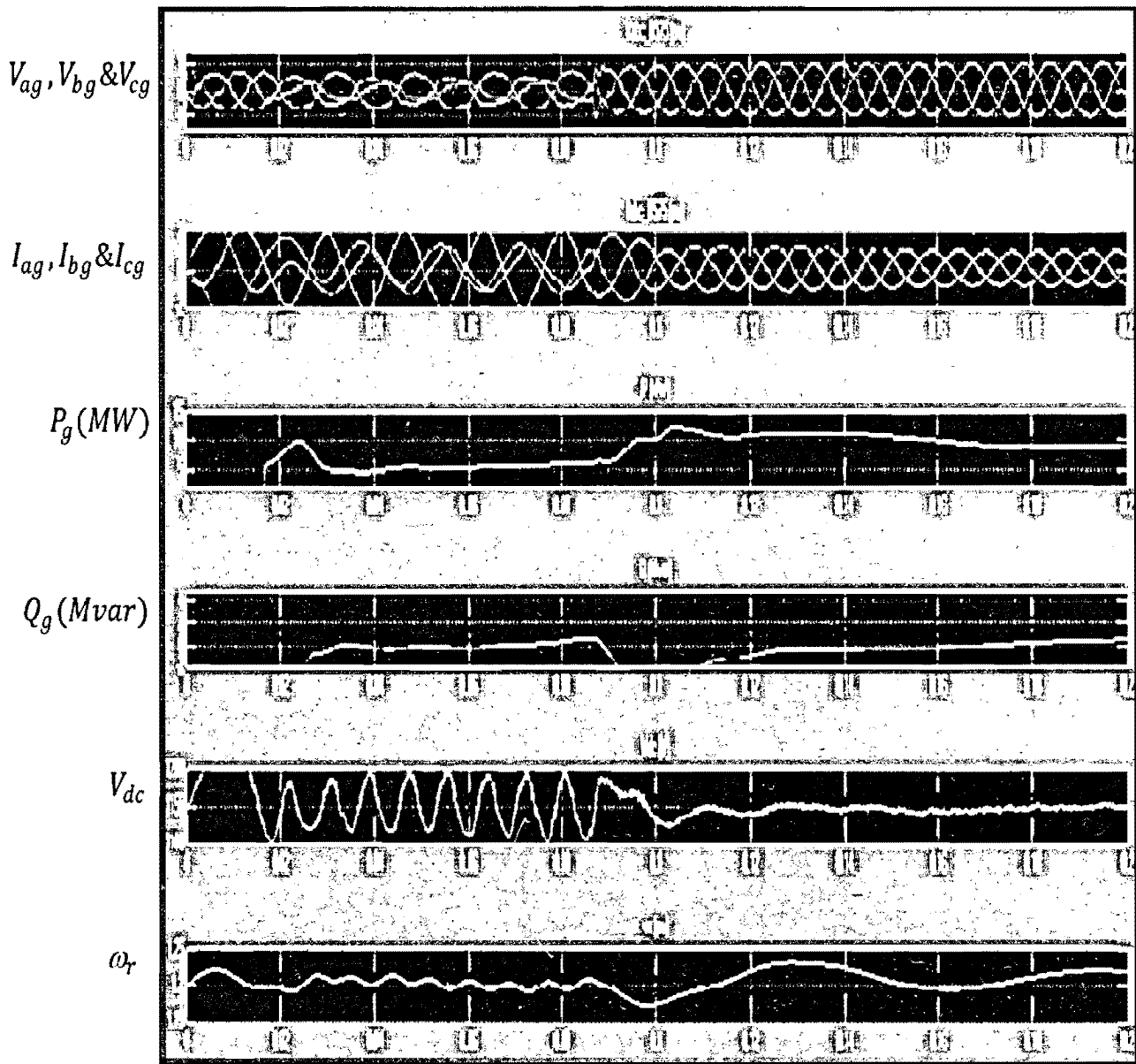


**Fig. 3-2 DFIG under unbalanced 2-phase fault.**

A two phase fault is applied to phase A and B of the transmission line between the transformer and B25 bus bar. This fault has caused severe disturbance in the DFIG behaviour as well as the entire network. As depicted in Fig. 3-2, the DC voltage is not stable anymore and far from the rated value with a lot of harmonics, this overvoltage DC can easily damage the capacitor. The active power was lost for significant time and when it returned it shows over production due to the power imbalance. It can be observed that, reactive power between  $t=0.02s$  to  $t=0.1s$  is not zero and it's injecting undesirable power to the network. The system recovers only around  $t=0.15s$ .

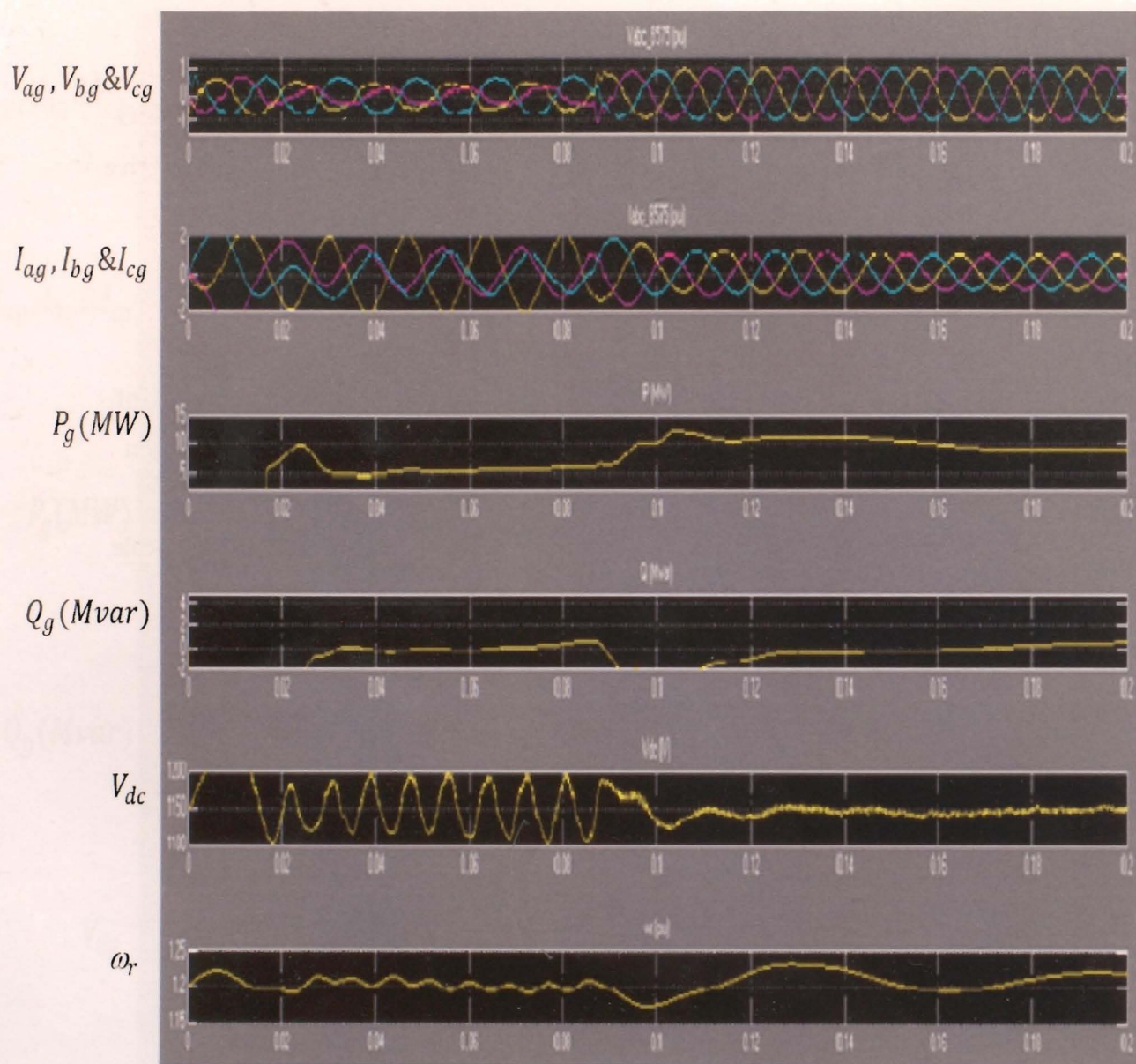


**Fig. 3-2 DFIG under unbalanced 2-phase fault.**

A two phase fault is applied to phase A and B of the transmission line between the transformer and B25 bus bar. This fault has caused severe disturbance in the DFIG behaviour as well as the entire network. As depicted in Fig. 3-2, the DC voltage is not stable anymore and far from the rated value with a lot of harmonics, this overvoltage DC can easily damage the capacitor. The active power was lost for significant time and when it returned it shows over production due to the power imbalance. It can be observed that, reactive power between  $t=0.02s$  to  $t=0.1s$  is not zero and it's injecting undesirable power to the network. The system recovers only around  $t=0.15s$ .

### 3.4 Summary

In this chapter the simulations of DFIG during various types of fault in the network were analyzed and presented. The dynamic response of the DFIG under fault was observed to be different and random in nature during the random fault occurrence in the power system. During the steady-state operation of the DFIG and its dynamic response to voltage sag resulting from a remote fault on the 120-kV system is plotted. The fault was introduced at the beginning and removed approximately after 0.1s. As a result; the DFIG wind farm produces lower power during the voltage sag. Following the voltage sag, as depicted in the previous sections, current, power and reactive power peaks have all exceeded their corresponding rated values. This could lead to entirely shut down of the system.

## CHAPTER 4

# FAULT DETECTION AND PROTECTION

### 4.1 Introduction

Grid codes require wind farms to stay connected and continue generation in the main system low voltage emergency conditions. Due to the limited capacity of converters, DFIG wind turbines may suffer from over rotor currents or over voltages in the DC-links. As a result, appropriate control and protection schemes must be applied. Modeling the fault current behaviour of DFIG will help to determine its dynamic performance and its possible impact on the power system. Different approaches have been taken by many software tools to model DFIG protection scheme and wind farms.

The following sections will discuss different active crowbar configurations, the fault detection method, the integration of the active crowbar system with the DFIG and the overall system behaviour under various fault conditions. This project report initially addresses the modeling considerations for an induction machine and then identifies the special considerations needed for a DFIG. A 9 MW wind farm with six units of 1.5 MW DFIG wind turbines is studied by creating symmetrical and asymmetrical faults in different zones. Voltage and current waveforms are presented and discussed during fault.

According to [17] commercial DFIG wind turbines demonstrate that the timing of deactivating crowbar and the value of the series resistor have critical effects on the converter safety and the system recovery. By use of a rotor crowbar connected with a series resistor and a modified control strategy on the grid-side converter, the DFIG wind turbine is capable of riding through voltage dips up to 15% without absorbing a lot of reactive power, which greatly contributes to the main system voltage recovery [16].

The fault ride-through capability is considered crucial for the system stability. It is commonly demanded from modern wind turbines, that they are not allowed to disconnect in case of faults.

One of the most often used variable speed configurations is to use an active crowbar fault ride through mechanism. Therefore, crowbar circuit is designed enabling the wind turbine to ride through transient faults. With the addition of crowbar the wind turbines can stay connected to the grid, maintain their generation capacity, and resume normal grid operation after the fault is cleared.

The following sections will discuss different active crowbar configurations, the fault detection method, the integration of the active crowbar system with the DFIG and the overall system behaviour under various fault conditions.

## 4.2 Fault Detection Methods

The fault detection methods investigated in this project play an important role in the independent active crowbar system. This active crowbar is connected to the rotor windings providing a bypass path for the rotor current under critical fault conditions. This section will focus on the methods of detection. The detailed model and methods of fault detection are not included in this project as it is above the scope of this project; however, the brief discussion for common methods is included.

Current measurement fault detection methods are used under fault conditions, the rotor current exceeds the converter rating substantially, which can be used for fault detection. The three-phase rotor currents are sensed and feed into detection block, where the currents are converted to the  $dq$  reference frame to have a faster response. The magnitude of current vector is compared to a reference value and fault indication is latched based on the equality [17].

The other fault detection method is using voltage RMS value of stator voltage. This method is mostly applied due to the high cost of the rotor current detection method. Fault usually appears as the voltage dip on the stator side. Then the stator voltages can be used to detect the fault. This method segregates the active crowbar independent from the turbine's control system. Also, fault detection using instantaneous pseudo-power detection used as an alternative to detect fault.

Three phase faults are much easier to detect through voltage magnitude in the synchronous  $dq$  rotating frame because the fault is balanced, the fault involves all three phases and contain the

same characteristics. Single phase and two phase faults are more difficult to detect as the voltage magnitude has a longer delay that may go undetected. The DFIG is capable of operating under these types of fault with no significant disturbance to the grid however it is not recommended.

Even though, the DFIG can run under single and two phase faults undetected, they do pose a serious problem to the rotor circuit and could possibly result in the network disturbance. Excessive rotor currents under these fault conditions will induce damage to the machine side VSC.

### 4.3 Protection Using Active Crowbar

In case of grid faults very high short circuit currents arise in the stator. These high transient currents are transferred to the rotor due to the inductive coupling between stator and rotor, implying a high damaging risk for the power electronics of the rotor side converter. Due to this reason a suitable protection of DFIG is necessary. A simple protection method is to short-circuit the rotor via an external rotor resistant called crowbar, when high rotor currents are detected. The crowbar coupling protects the converter system and facilitates fault ride through, which enables the DFIG to contribute to power supply directly after fault clearing. When the crowbar protection is triggered, the rotor side converter is blocked and the DFIG behaves as a squirrel cage induction generator. This implies that the whole controllability of the DFIG is lost during crowbar coupling.

The control strategy adopted during fault for this analysis is described: the RSC is blocked and the crowbar system is activated; the GSC controls the DC-link voltage; the RSC is restarted and crowbar system is removed after the fault elimination. Different  $R_{\text{crow}}$  are analyzed (2, 5 and 10 times the original rotor resistance  $R_r$ ) [14]. This is the most common operation mode during faults for countries with no reactive current injection requirement. Considering the stability of the machine the desired rotor speed should be as closer as possible to the normal operation speed in order to avoid the critical rotor speed, as described in Section 3. The active power injected by the DFIG is also increased for high values of the  $R_{\text{crow}}$ , as explained in [14].

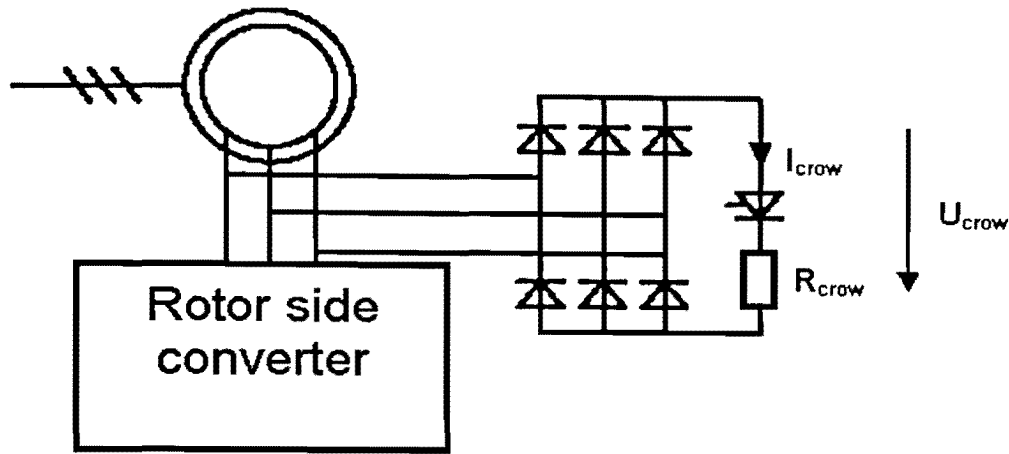


Fig. 4-1 Diode bridge crowbar.

The crowbar circuit that was used in simulations consists of a diode bridge that rectifies the rotor phase currents and a single thyristor in series with resistance  $R_{crow}$  as it is depicted in Fig 4-1.

The crowbar doesn't work in chopper mode. The thyristor is turned on when the DC link voltage  $U_{dc}$  reaches its maximum value

$$U_{dc} \geq U_{dc \max} \quad (4.1)$$

Simultaneously the rotor circuit is disconnected from the rotor side frequency converter and connected to the crowbar. The rotor remains connected to the crowbar until the main circuit breaker disconnects the stator from the network. The rectified current  $I_{crow}$  can be calculated from DFIG rotor currents as

$$I_{crow} = \frac{(|I_{ra}| - I_{ra} + |I_{rb}| - I_{rb} + |I_{rc}| - I_{rc})}{2} \quad (4.2)$$

The dc voltage over the crowbar  $U_{crow}$  is calculated as

$$U_{crow} = R_{crow} I_{crow} - U_{CB\_semic} \quad (4.3)$$

Where  $U_{CB\_semic}$  denotes the voltage drop over the thyristor.

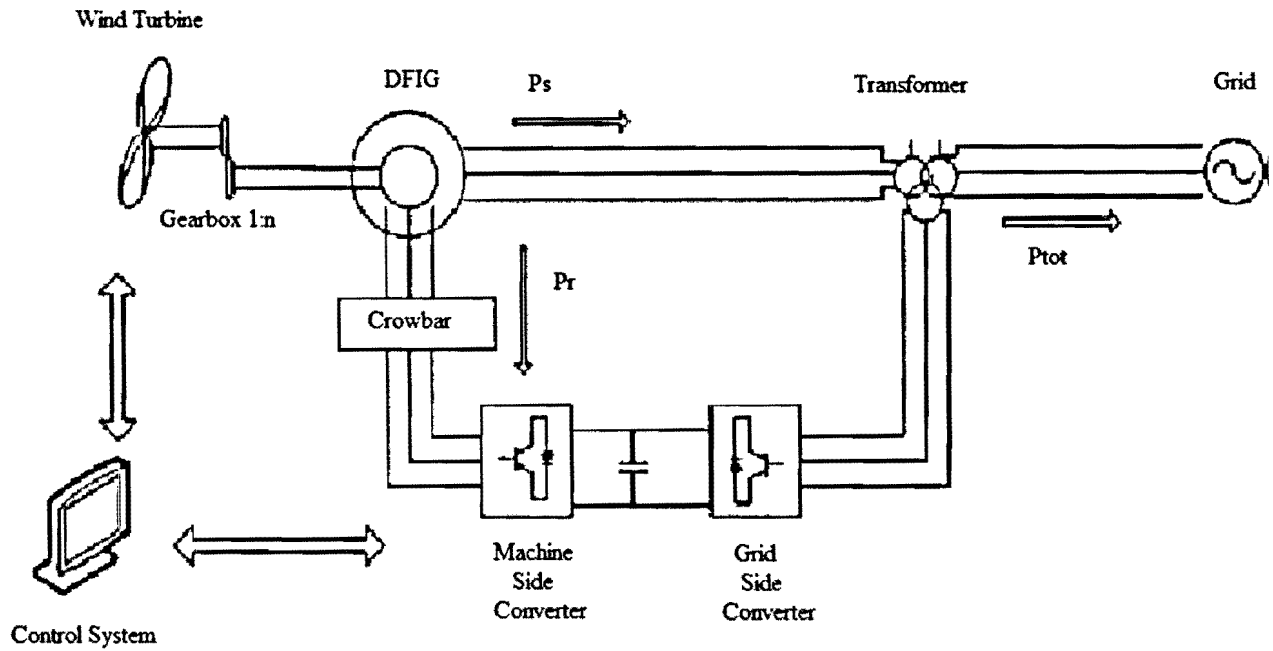


**Fig. 4-2 DFIG structure with active crowbar.**

The active crowbar is connected between the rotor of DFIG and rotor-side inverter, as it is depicted in (Fig 4.2). In contrast to the conventional crowbar, the active crowbar is fully controllable. A typical ride-through sequence [18] starts when the grid voltage decreases rapidly to a low level. This causes high current transients both in the generator stator and rotor. If either the rotor current or dc-link voltage levels exceed their limits, the IGBTs of the rotor-side inverter are blocked, and the active crowbar is turned on. The crowbar resistor voltage and the dc-link voltage are monitored during the crowbar operation. When these both voltages are low enough, the crowbar is turned off. After a short delay, for the rotor currents decay, the rotor-side inverter is restarted, and the reactive current component of the generator is ramped up in order to support the grid [16]. Naturally, the crowbar will be turned on again if a too-high rotor current or dc-link voltage is encountered after the turn off of the crowbar. This is often the case with severe two-phase faults that have a high negative-sequence voltage component in the stator. The negative sequence component has a high rotor slip [16]. Thus, very high voltages are induced in the rotor windings that make it impossible to control the rotor current with the available dc-link voltage. Thus, for the most severe unsymmetrical grid faults, the rotor-side inverter cannot be started before the fault has been cleared. Figure 4.2 illustrates the common control scheme of the DFIG coupled with a crowbar as discussed in this section.



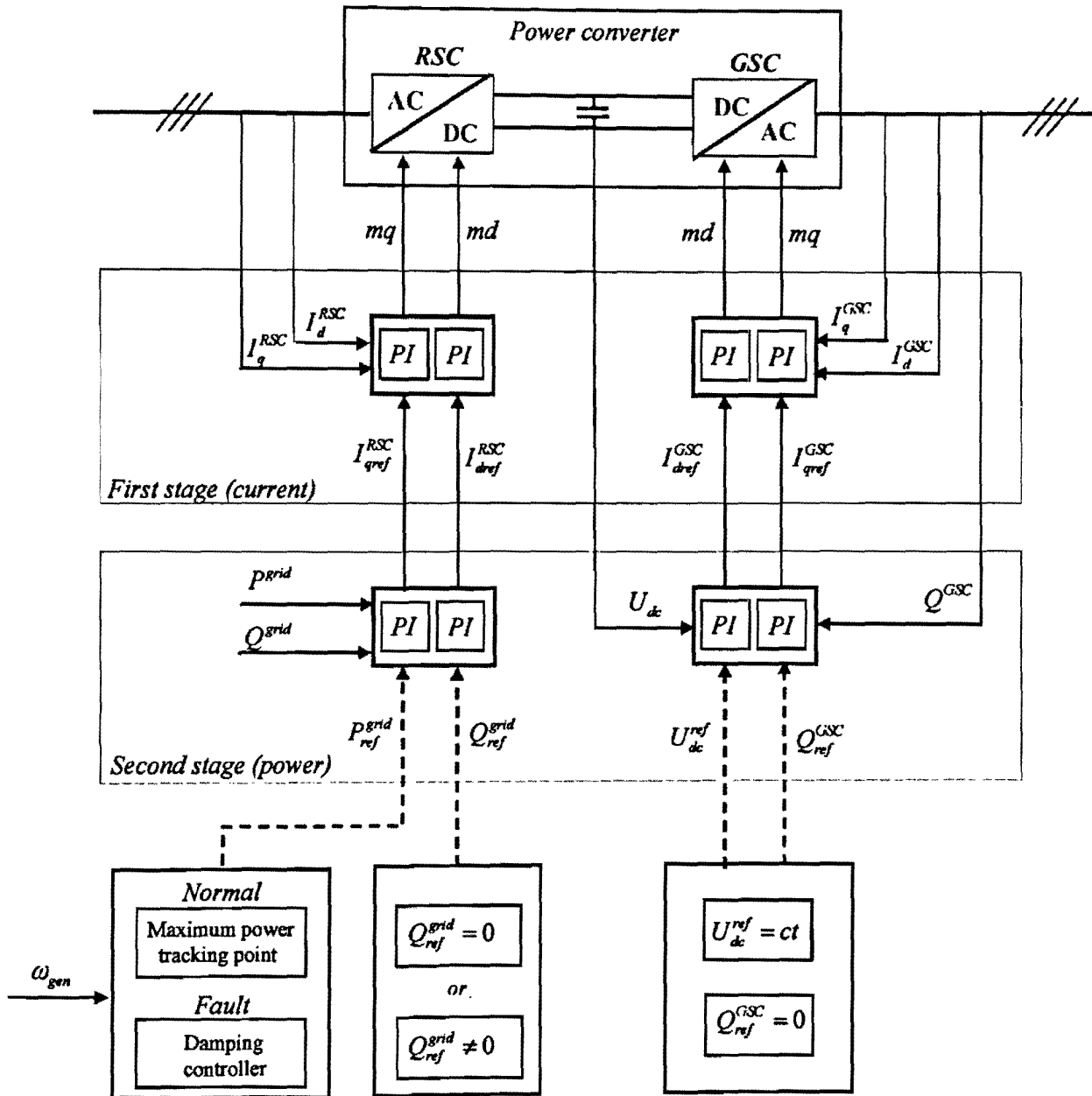


Fig. 4-3 control block of DFIG with a crowbar.

The DFIG control, illustrated in Fig 4.3, contains the electrical control of the power converters with block diagram of the main components. It is essential for the DFIG behaviour both in normal operation and during fault conditions. The control performance of the DFIG is very good in normal grid conditions allowing active and reactive power changes in the range of few

milliseconds. DFIG control can, within limits, hold the electrical power constant in spite of fluctuating wind, storing thus temporarily the rapid fluctuations in power as kinetic energy [18]. In Fig 4.3, the set point signals for the second stage controllers are also depicted. The reactive power set – point,  $Q_{ref}^{grid}$ , for the RSC can be set to a certain value or zero according to whether or not the DFIG wind turbine is required to contribute with reactive power. The GSC is usually reactive power neutral, namely its set-point of reactive power,  $Q_{ref}^{GSC}$ , is set to zero. This implies the GSC only exchanges active power with the grid, and therefore the transmission of reactive power from DFIG to the grid is done only through the stator. The reference signal for the dc voltage  $U_{dc}$  is set to a constant value, independent on the wind turbine operation mode. This value is mainly dependent on size of the converter, the stator – rotor ratio and the modulation factor of the power converter [8 9].

A three phase short circuit has been introduced at time instant 5 s. The transient stator current, rotor current and electromagnetic torque when the crowbar is not implemented are depicted in Fig 4-4 and in the detail Fig 4-5. The detailed plot of stator, rotor and DC-link voltages are shown in Fig 4-6[14].

Due to the resulting high transient in currents in the rotor with a peak value more than 3.5 p.u., the DC link by turning off all positive side IGBTs and turning on all negative side IGBTs thus short circuiting the rotor [17]. The electromagnetic torque due to the transients in the rotor and stator first increases in negative direction down to -1.8 pu, then rapidly rises to in the positive direction up to 1.6 pu. and then starts oscillation. At the time instance 5.13s, the stator of DFIG is disconnected from the network by opening the main circuit breaker because the network faults remains.

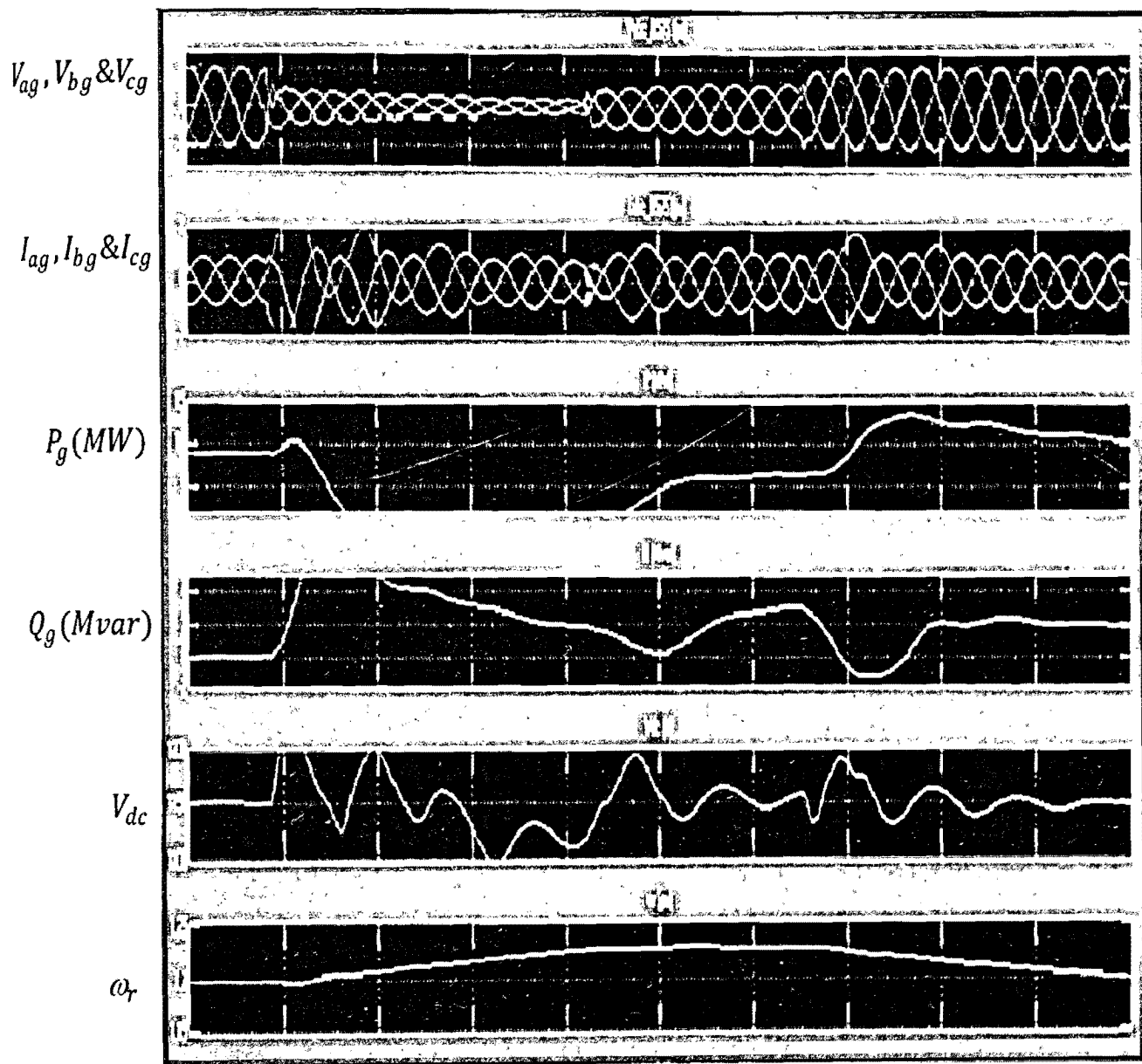


**Fig. 4-4 DFIG during Fault without Crowbar.**

The three phase fault is applied on a transmission line at B575 collector bus. The instant the fault introduced, the three phase voltages becomes out of phase with respect to each other as it can be observed on Figure (4-4). The three phase rotor current is very high at starting; this is in the range approximately three times the rating current, which can easily destroy the converter. The active power  $P$  decreases by significant factor as a result of the fault impedance. On the other

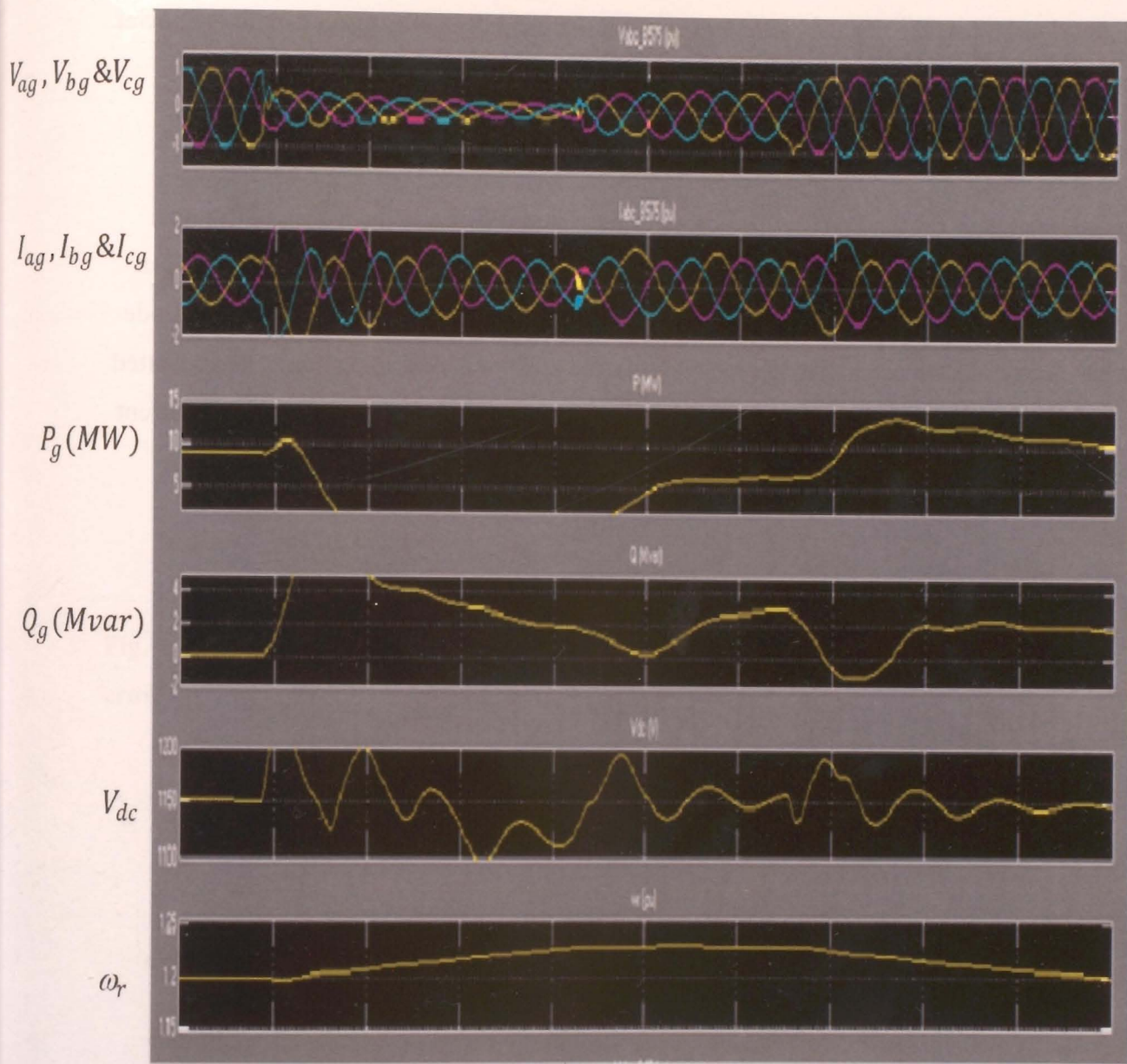


**Fig. 4-4 DFIG during Fault without Crowbar.**

The three phase fault is applied on a transmission line at B575 collector bus. The instant the fault introduced, the three phase voltages becomes out of phase with respect to each other as it can be observed on Figure (4-4). The three phase rotor current is very high at starting; this is in the range approximately three times the rating current, which can easily destroy the converter. The active power  $P$  decreases by significant factor as a result of the fault impedance. On the other

side, from Figure (4-4) the changes of reactive power are insignificant compared to active power characteristics.

The simulation result for the DFIG with a crowbar activated is given in the following figures with the detailed description of each rotor currents and DC voltage characteristics. Similarly in the previous case the 3-phase short circuit has been introduced at the time instant 5 s. The diode bridge has been modeled according the model given the beginning of this chapter. The simulated transient stator current, rotor current and electromagnetic torque, when the crowbar over-current protection is implemented are depicted in Fig 4-7[14].

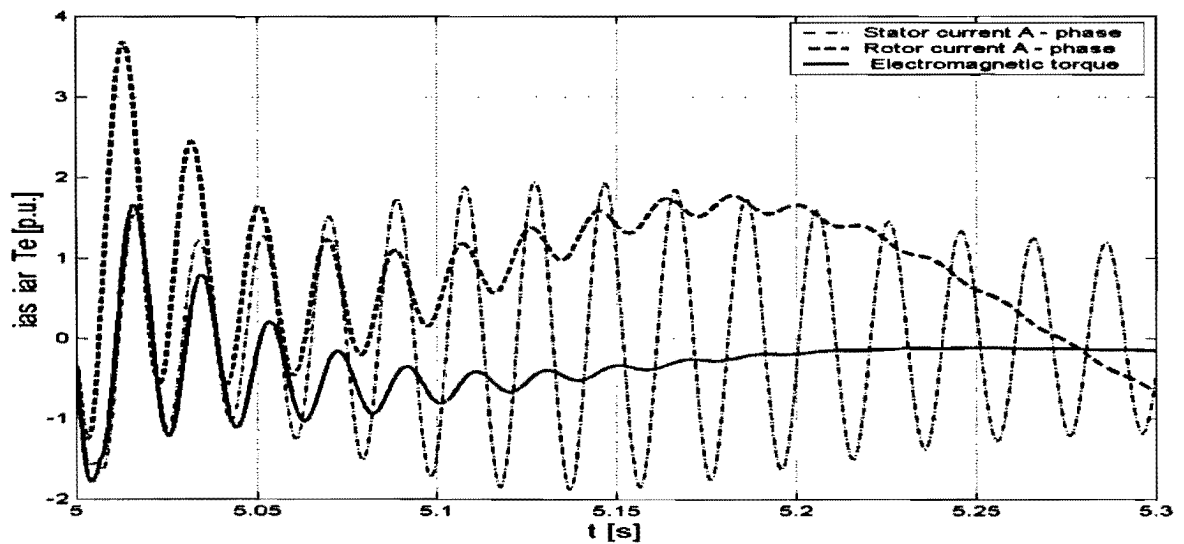


**Fig. 4-5 stator current, rotor current and electromagnetic torque during fault without crowbar[14].**



side, from Figure (4-4) the changes of reactive power are insignificant compared to active power characteristics.

The simulation result for the DFIG with a crowbar activated is given in the following figures with the detailed description of each rotor currents and DC voltage characteristics. Similarly in the previous case the 3-phase short circuit has been introduced at the time instant 5 s. The diode bridge has been modeled according the model given the beginning of this chapter. The simulated transient stator current, rotor current and electromagnetic torque, when the crowbar over-current protection is implemented are depicted in Fig 4-7[14].

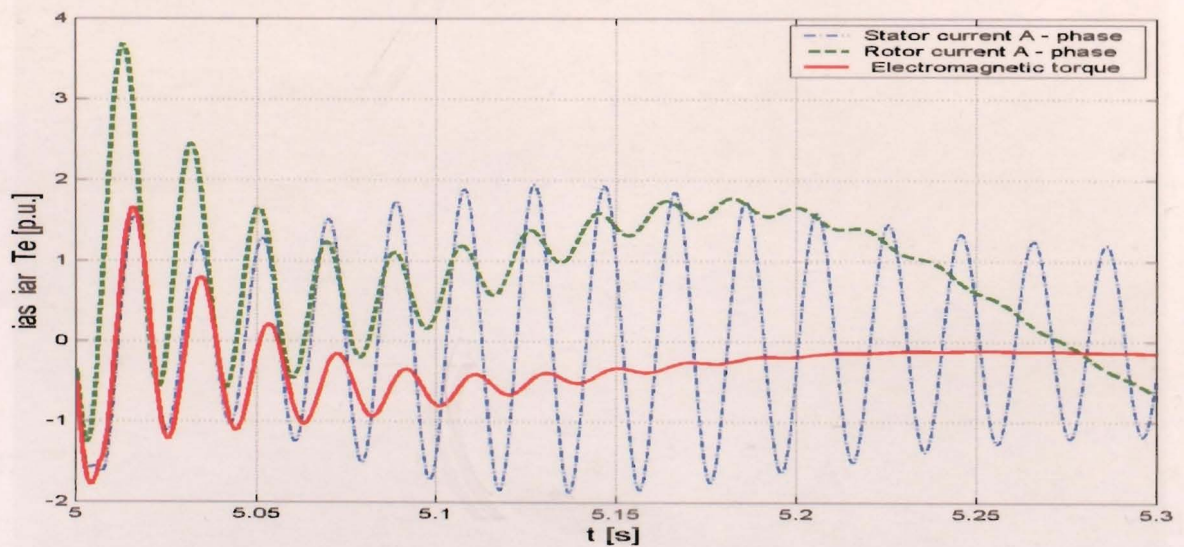


**Fig. 4-5 stator current, rotor current and electromagnetic torque during fault without crowbar[14].**

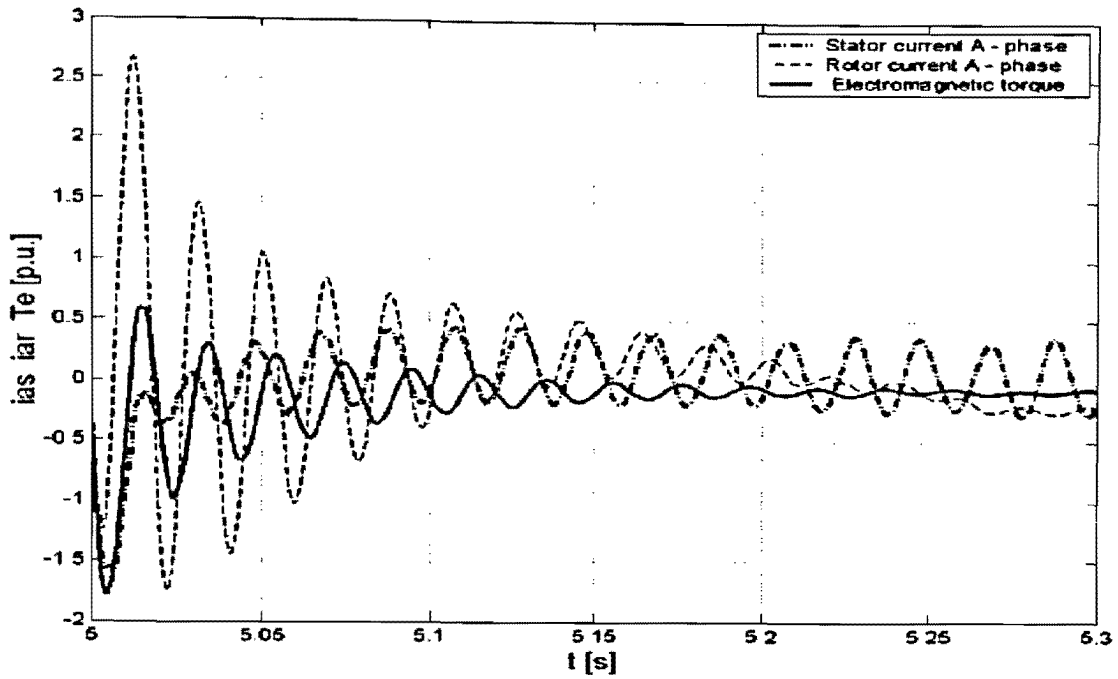


Fig. 4-6 stator current, rotor current and electromagnetic torque during fault with crowbar[14].

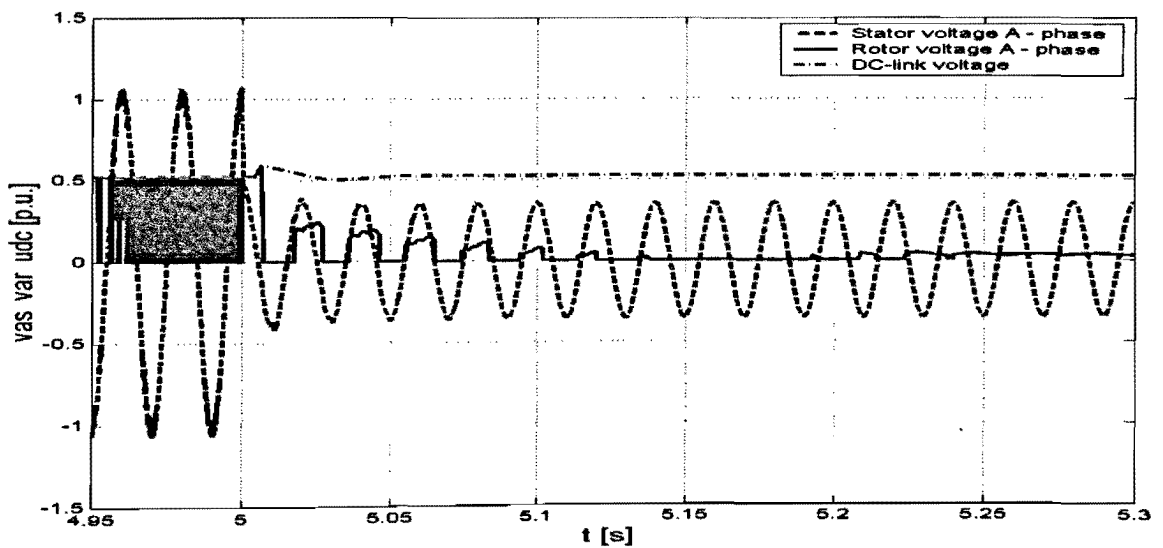


Fig. 4-7 Stator voltage rotor voltage and DC-link voltage during network disturbance with the crowbar implemented.

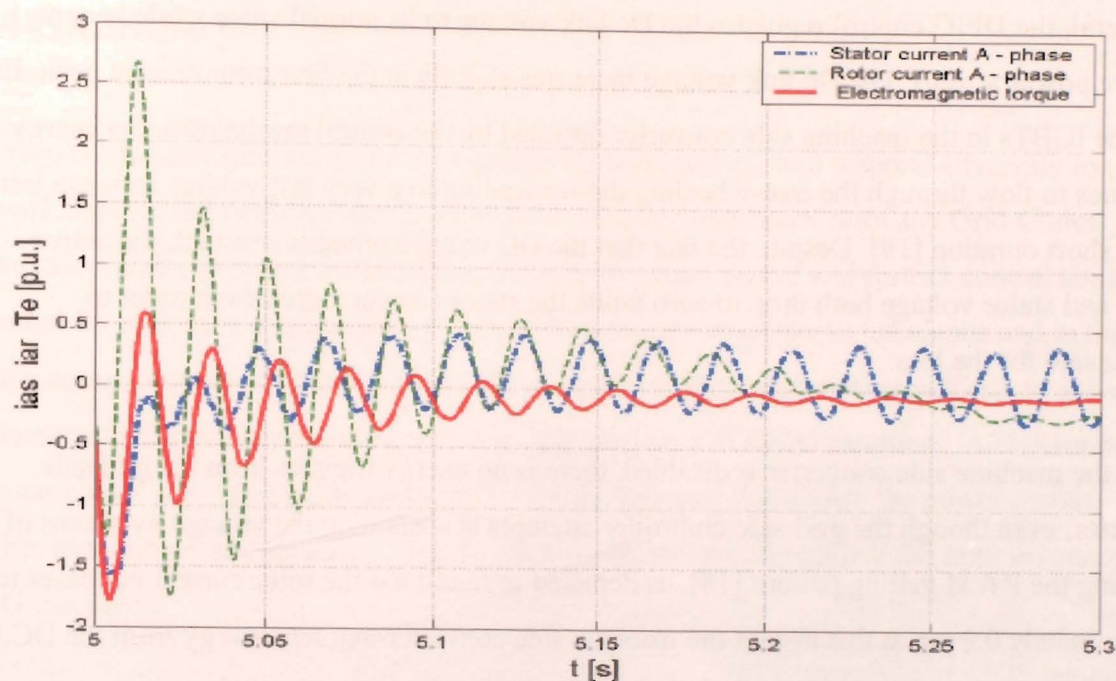


Fig. 4-6 stator current, rotor current and electromagnetic torque during fault with crowbar[14].

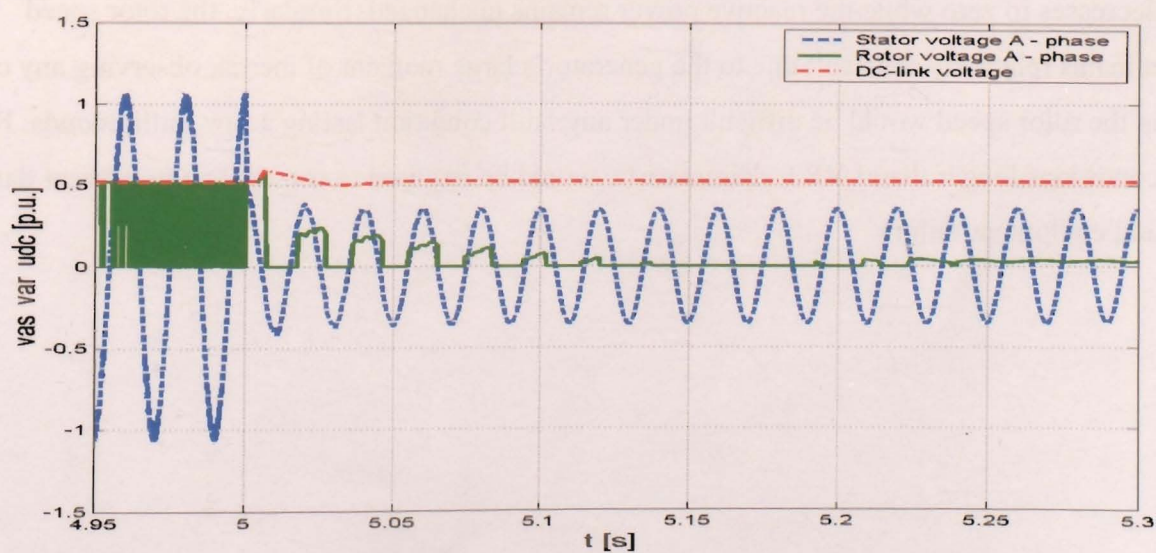


Fig. 4-7 Stator voltage rotor voltage and DC-link voltage during network disturbance with the crowbar implemented.



In general, the DFIG control regulates the Dc link voltage to its normal value while keeping reactive power at zero. The Dc link voltage increases slightly at the first rotor current peak. Even with the IGBTs in the machine side converter disabled by the control mechanism, the energy continues to flow through the free-wheeling diodes leading to a very fast voltage increase lasting a very short duration [18]. Despite the fact that the DC voltage remains constant, the active power and stator voltage both drop to zero while the stator current increases in order to compensate for the loss.

When the machine side converter is disabled, there is no energy transfer from the grid side converter, even though the grid side controller attempts at sustaining the voltage by means of adjusting the PWM getting pattern [18], as depicted in figure 4.4 the rotor current increases to approximately 0.8 pu, at this instant the machine side converter extracts energy from the DC link capacitor.

The overall system performance of the DFIG with the active crowbar under different fault condition does not drastically impede the system behaviour as well, has no negative impact on the grid or connected loads. Loads connected to generating systems that experience such faults have a tendency of drawing reactive power as a result of the impedance along the line and the generation system under such conditions, however in the simulation result, active power decreases to zero while the reactive power remains unchanged. Similarly, the rotor speed remains relatively constant; due to the generator's large moment of inertia, observing any change in the rotor speed would be difficult under any fault condition lasting a few milliseconds. Fault conditions longer than LVRT characteristic would be required to trip off line to prevent damage and equipment failure.

## 4. 4 Summary

The results obtained indicate that a standard DFIG wind turbine will respond adversely to network faults if not modified and is unlikely to achieve compliance with any Grid Codes. Unbalanced faults introduce sustained oscillations to output power and restrict control ability. Potential for controller improvements exist in damping the response to unbalance and in the re-connection response of the converters. Such improvements are however unlikely to solve the fundamental problems surrounding network fault tolerance of DFIG machines. A resistor bank crowbar circuit may protect the converters but they may also destabilise the power output. Further topological modifications must be considered in order to improve the fault tolerance of DFIG machines.

# CHAPTER 5

## CONCLUSION

### 5.1 Conclusion

Currently, the wind energy is one of the most promising renewable energy sources; it has been seen fast growing worldwide. The energy in wind is extracted by wind turbine and converted by generator into electrical energy, feeding the existing power system. Wind Energy Conversion Systems (WECS) convert the energy in moving air (the wind) to electrical energy. The basic idea is quite simple and has been around for centuries: the wind strikes some sort of set of blades mounted on a shaft that is free to rotate. The wind hitting the blades generates a force that turns the shaft, and this rotational kinetic energy may then be used for any of a number of purposes (historically, things like pumping water, moving a saw, or turning grain-grinding stones, to name a few). In a WECS, the rotating shaft turns an electric generator that converts the rotational kinetic energy to electric energy.

Variable speed doubly-fed induction generator based wind energy conversion system has dominant the variable speed wind energy system in the last ten years. Many systems have been installed and the penetration rate of wind energy is increasing every year.

Low Voltage Ride Through for Wind Turbines with DFIG is a challenge that all manufacturers must solve. Most manufacturers have already implemented LVRT systems, but compliance of the different grid codes is still a problem that has not been totally solved. New LVRT systems must comply grid codes without penalizing the system cost. The ideal solution is the utilization of low cost additional hardware (active crowbar) and adaptation of control strategies.

The DFIG based WECS can be upgraded inside the control system, where the rotor current is detected and active crowbar is employed to short the rotor circuit, in order to by-pass the excessive rotor energy to crowbar resistance. The machine side converter can be protected by disabling the gating signal when the crowbar is activated. The solution can be done by upgrading or in the newly designed system. In this project, an active crowbar for low voltage ride through

protection method is proposed. Also the novel fault detection method based IPPD is recommended. The method has fast response than other detection methods, which can also be used to detect different faults, balanced or non-balanced effectively. This method is used with stand alone crowbar to avoid the expensive system upgrade. The simulation results verified the proposed protection for DFIG and rotor side converter.

## 5.2 Major Contribution

In this project, the major contribution is the low voltage ride through protection scheme for DFIG with a better response and considerably cheaper Crowbar to protect rotor side converter from an excessive current. Crowbar is an effective solution for fault ride through in DFIG based wind energy system. However, it needs the upgrade of control system or new design. The problems existed that in the traditional fault detection methods through stator voltage have the one cycle time delay and sometimes are not suitable for unbalanced faults. The proposed crowbar protection is verified through simulation that is effective to protect the machine side converter from over current, which enable the WECS ride through the fault under any circumstances.

## REFERENCES

- [1] Global Wind Energy Council. (2009, February.) “Global Wind Energy Markets Continue to Boom” [Online]. <http://www.gwee.net/>
- [2] Canadian Wind Energy Association, CAWEA. “Growing wind Energy market”, April, 2010; [http://www.canwea.ca/wind-energy/supplychain\\_e.php](http://www.canwea.ca/wind-energy/supplychain_e.php)
- [3] American Wind Energy Association (AWEA). “Annual Wind Energy Report, 2009” [http://www.awea.org/reports/Annual\\_Market\\_Report\\_Press\\_Release\\_Teaser.pdf](http://www.awea.org/reports/Annual_Market_Report_Press_Release_Teaser.pdf)
- [4] World Wind Energy Association (WWEA) <http://www.windea.org/technology/ch01/estructura-en.htm>
- [5] The Solar Guide. “Wind Power” <http://www.thesolarguide.com/wind-power/>
- [6] Andreas Petersson, “Analysis, Modeling and Control of Doubly – Fed Induction Generators for Wind Turbines”; PhD Theses, Chalmers University of Technology, Gutenberg, Sweden, 2005
- [7] Anca D. Hansen, Gabriele Michalke, “Fault ride-through capability of DFIG wind turbines”, Renewable Energy 32 (2007) 1594-1610
- [8] J. B. Ekanyake, L. Holdsworth, X. G. Wu and N. Jenkins, “Dynamic modeling of doubly fed induction generator wind turbines”, IEEE Transactions on Power Systems, vol. 18(1), February 2003, pp. 790-810
- [9] Ted Brekken, Ned Mohan, “A Novel Doubly-fed Induction Wind Generator Control Scheme for Reactive Power”, Dept OF Electrical Engineering, University Of Minnesota, Minneapolis, MN 55455 USA
- [10] M. Dubois, H. Polinder and J. A. Ferreira, “Comparison of generator topologies for direct drive wind turbines”, in Proceedings NORPIE, 2000, pp. 20-26
- [11] Martinez De Alegria, J.L. Villate, J. Andreu, I. Gabiola and P. Ibanez, “GRID CONNECTION OF DOUBLY FED INDUCTION GENERATOR WIND TURBINES”, Bilbao, Spain, 2008
- [12] R. Pena, J. C. Clare and G. M. Asher, “Doubly fed induction generator using back-to-back PWM converters and its application to variable-speed wind-energy generation”, in Proceedings Electrical Power Applications, vol. 143, 1996, P. 231-242

- [13] S. Seman, J. Niiranen, S. Kanerva, and A. Arkkio, "Analysis of 1.7 MVA Doubly Fed Wind-Power Induction Generator during Power Systems Disturbances", IEEE Transactions on Power Systems, 2006
- [14] Seman, S., Niiranen, J., Arkkio, A. 2006. "Ride-Through Analysis of Doubly Fed Induction Wind-Power Generator under Unsymmetrical Network Disturbance", IEEE Transaction on Power Systems, Accepted for future publication, 7 p
- [15] G. Tsourakis and C. D. Vourns, "Simulation of Low Voltage Ride Through Capability of Wind Turbines with DFIG",
- [16] S. R. Pena, J. C. Clare, and G. M. Asher, "Doubly fed induction generator using back-to-back PWM converters and its application to variable-speed wind-energy generation," Proc. Inst. Elect. Eng., Elect. Power Appl., vol. 143, no. 3, pp. 231–241, May 1996.
- [17] Jouko Niiranen, Slavomir Seman, Jari-Pekka Matsinen, Reijo Virtanen and Antti Vilhunen; "Low voltage Ride Through Testing of Wind Turbine Drives", ABB, 2nd Edition of IEC61400-21
- [18] Rabelo, B.; Clare, J.C; Asher, G.M.; Doubly fed induction generator using back-to-back PWM converters and its application to variable speed wind-energy generation; IEEE Proceedings on Electrical Power Application, Vol.143, No. 3, 1996
- [19] Investigation of different Methods to Control a Small Variable – Speed Wind Turbine with PMSM Drives; Journal of Energy Resources Technology, Vol. 129, No. 3, 2007
- [20] Protsenko, K.; "Flexible Power Flow Control for Brushless Doubly Fed Induction Generator"; Thesis, Ryerson University, Toronto, Ontario, 2007
- [21] Ramroop, A.D Shoba; "Fault Detection of Fault Ride Through for Doubly-Fed Induction Generator Based Wind Energy Systems"; Thesis, Ryerson University, Toronto, Ontario, 2008
- [22] A. Petersson, L. Harnefors and T. Thiringer, "Comparison between stator-flux and grid-flux-oriented rotor current control of doubly-fed induction generators", *Proceedings of the 35th Annual IEEE Power Electronics Specialists Conference – PESC'04*. Volume 1, 20-25 June 2004 pp. 482 - 486
- [23] Tanuj Mishra; "Dynamic Performance Estimation of DFIG wind turbine under Balance /Unbalance grid fault condition", Thesis, National Institute of Technology, Rourkela

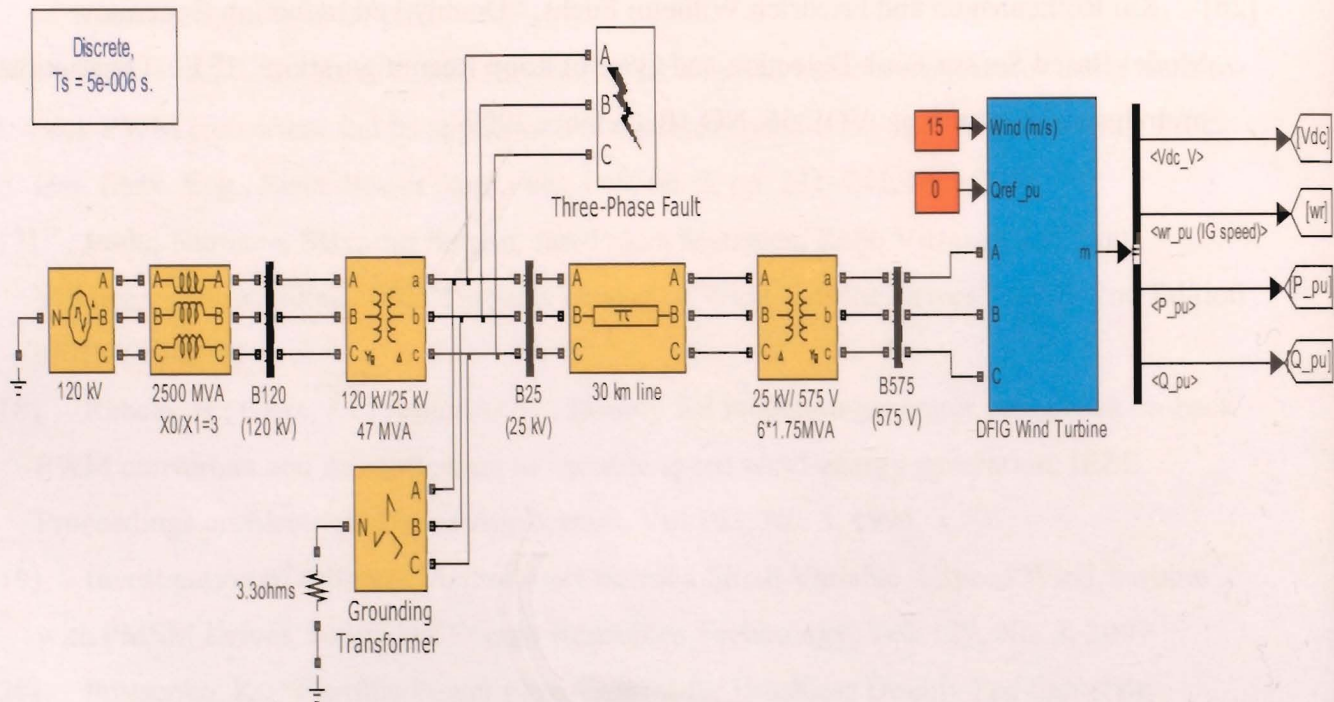
- [24] Gavin J. Armstrong, et al. "A Comparison Of Estimation Techniques For Sensor less Vector Controlled Induction Motor Drives" Dept. Electrical & Electronic Engineering University of Newcastle-upon-Tyne Newcastle-upon-Tyne, NE1 7RU - United Kingdom
- [25] M. Tsili, Ch. Patdiouras and S. Papathanassiou; "Grid Code Requirements for Large wind Farms: A Review of Technical Regulations and Available Wind Turbine Technologies" National Technical University of Athens (NTUA) School of Electrical and Computer Engineering, Athens, Greece
- [26] Kai Rothenhagen and Friedrich Wilhelm Fuchs; "Doubly Fed Induction Generator Model-Based Sensor Fault Detection and Control Loop Reconfiguration", IEEE Transactions on Industrial Electronics. VOL.56. NO.10. October 2009



# Appendices

## Appendix A

Modiefied Simpowersystems wind farm and DFIG Simulink model with back to back converters



# Appendix B

